# MONITORING STRATIFICATION AND CURRENTS AT THE CONTINENTAL SLOPE OF THE SCOTIA SEA, ANTARCTICA

A Senior Scholars Thesis

by

MELANIE R. THORNTON

Submitted to the Office of Undergraduate Research
Texas A&M University
in partial fulfillment of the requirements for the designation as

UNDERGRADUATE RESEARCH SCHOLAR

April 2011

Major: Environmental Geoscience

# MONITORING STRATIFICATION AND CURRENTS AT THE CONTINENTAL SLOPE OF THE SCOTIA SEA, ANTARCTICA

A Senior Scholars Thesis

by

MELANIE R. THORNTON

Submitted to the Office of Undergraduate Research
Texas A&M University
in partial fulfillment of the requirements for the designation as

UNDERGRADUATE RESEARCH SCHOLAR

Approved by:

Research Advisor: Alejandro H. Orsi
Director for Honors and Undergraduate Research: Sumana Datta

April 2011

Major: Environmental Geoscience

# ABSTRACT

Monitoring Stratification and Currents at the Continental Slope of the Scotia Sea, Antarctica. (April 2011)

Melanie R. Thornton
Department of Oceanography
Texas A&M University

Research Advisor: Dr. Alejandro H. Orsi
Department of Oceanography

The most notable mixing that takes place in the Southern Ocean exists when the Antarctic Circumpolar Current (ACC) encounters abrupt changes in the ocean floor topography. Therefore, the spatial and vertical distribution of mixing in the southern Scotia Sea is fundamental to fully understanding the rapid ventilation of the Circumpolar Deep Water (CDW) in an area where the ACC readily interacts with the Antarctic Slope Current (ASC). The objective of this study is to describe the dramatic freshening and cooling of CDW at the northern flank of the South Scotia Ridge (SSR) near 53°W, a study area during the ACROSS program of the International Polar Year. It is aimed at understanding how the deep ocean is more directly ventilated along intermediate density layers, which can rapidly transmit climate-related changes observed in the colder Antarctic slope waters to the rest of the world deep ocean.

Two ACROSS moorings (M1 and M2) were deployed in February 2009 at the slope of the SSR near 53°W to directly measure velocity and physical properties at the ASC. M1

was located at 600 m water depths, and M2 at 1800 m, with a total of nine current meters and fourteen Temperature-Conductivity-Pressure recorders set approximately 100-200 m apart from each other on the line. All instruments were recovered in January 2010.

The major water masses found within the study area are: Antarctic Surface Water, modified CDW, and deep and bottom waters.

The record-length mean velocity field is dominated by a strong (> 20 cm $s^{-1}$) southwestward current at the upper slope, the ASC. Intrusions of the ACC are evident throughout the record. When the ACC impinges on the SSR, slope-modified CDW is formed by the local mixing between ventilated slope water from the Weddell Sea and Bransfield Straits and CDW from the Scotia Sea.

Outflow of MCDW to the abyssal Scotia Sea is facilitated by energetic frontal interactions with the SSR. The associated intermediate-depth export of slope waters by this active mechanism is relevant to the Meridional Overturning Circulation, thus it contributes to the large-scale redistribution of ocean heat that couples Antarctic convention to global climate.

# DEDICATION

This thesis is dedicated to my parents, John and Diane Thornton.

# ACKNOWLEDGMENTS

I owe the completion of this thesis to many individuals. I would like to thank National Science Foundation, whose funding for the Antarctic CRossroad Of Slope Streams (ACROSS) under OCE-0961523 made this research possible.

I want to thank my research advisor, Dr. Alejandro H. Orsi, for his assistance and guidance in the development of my research, and for giving me the opportunity to research as an undergraduate student. I would especially like to acknowledge Chrissy Wiederwohl for her constant assistance and guidance throughout this research project. I truly appreciate her support, laughter, advice and MATLAB expertise, and without her assistance this research would be indescribable. I would also like to thank my co-worker, Yong Sun Kim, for his insight in examining the data used in writing this document.

I would like to thank my academic advisor, Emily Dykes, for informing me about this research opportunity. I owe my gratitude to her for continuous aid and inspiration of undergraduates, including me, in the Environmental Program.

Above all, I want to thank my family for their encouragement and support of my research. I am fortunate to have parents, siblings, aunts, uncles and grandparents that support me in all possible ways. They have motivated me to accomplish anything that lies ahead in my life.

# NOMENCLATURE

| | |
|---|---|
| AABW | Antarctic Bottom Water |
| ACC | Antarctic Circumpolar Current |
| ACROSS | Antarctic Crossroad of Slope Streams |
| ASC | Antarctic Slope Current |
| ASF | Antarctic Slope Front |
| CDW | Circumpolar Deep Water |
| CTD | Conductivity, Temperature, Depth |
| ESASSI | España Synoptic Antarctic Shelf-Slope Interactions |
| IPY | International Polar Year |
| LADCP | Lowered Acoustic Doppler Current Profiler |
| LCDW | Lower Circumpolar Deep Water |
| MCDW | Modified Circumpolar Deep Water |
| MOC | Meridional Overturning Circulation |
| NSF | National Science Foundation |
| SASSI | Synoptic Antarctic Shelf-Slope Interactions |
| SBE | Sea-Bird Electronics |
| SSR | South Scotia Ridge |
| TCP | Temperature-Conductivity-Pressure |
| UCDW | Upper Circumpolar Deep Water |
| XBT | Expendable Bathythermograph |

# TABLE OF CONTENTS

Page

# LIST OF FIGURES

FIGURE Page

# LIST OF TABLES

# CHAPTER I

# INTRODUCTION

## Research interest

The Southern Ocean hosts a multitude of water masses that play a significant role in the global Meridional Overturning Circulation (MOC) and its circulation has the unique ability to export these water masses throughout the global ocean. The resulting large-scale redistribution of ocean heat couples Antarctic convention to global climate. Thus the long-term goal of this study is to better understand the Southern Ocean contribution to climate.

The objective of this study is to describe the rapid freshening and cooling of Circumpolar Deep Water (CDW) at a unique location around Antarctica (Figure 1). This site (Figure 1) is where the eastward-flowing Antarctic Circumpolar Current (ACC) interacts with the Antarctic Slope Current (ASC) that had entered the Scotia Sea from the Weddell Sea, across the western South Scotia Ridge. This research project aims to improve the understanding on how the deep ocean is ventilated along intermediate density layers by slope waters exported near the tip of the Antarctic Peninsula. It will determine a direct mechanism that can rapidly transmit climate-related changes observed in the colder coastal waters to the deep ocean.

---

This thesis follows the style of *Journal of Geophysical Research*.

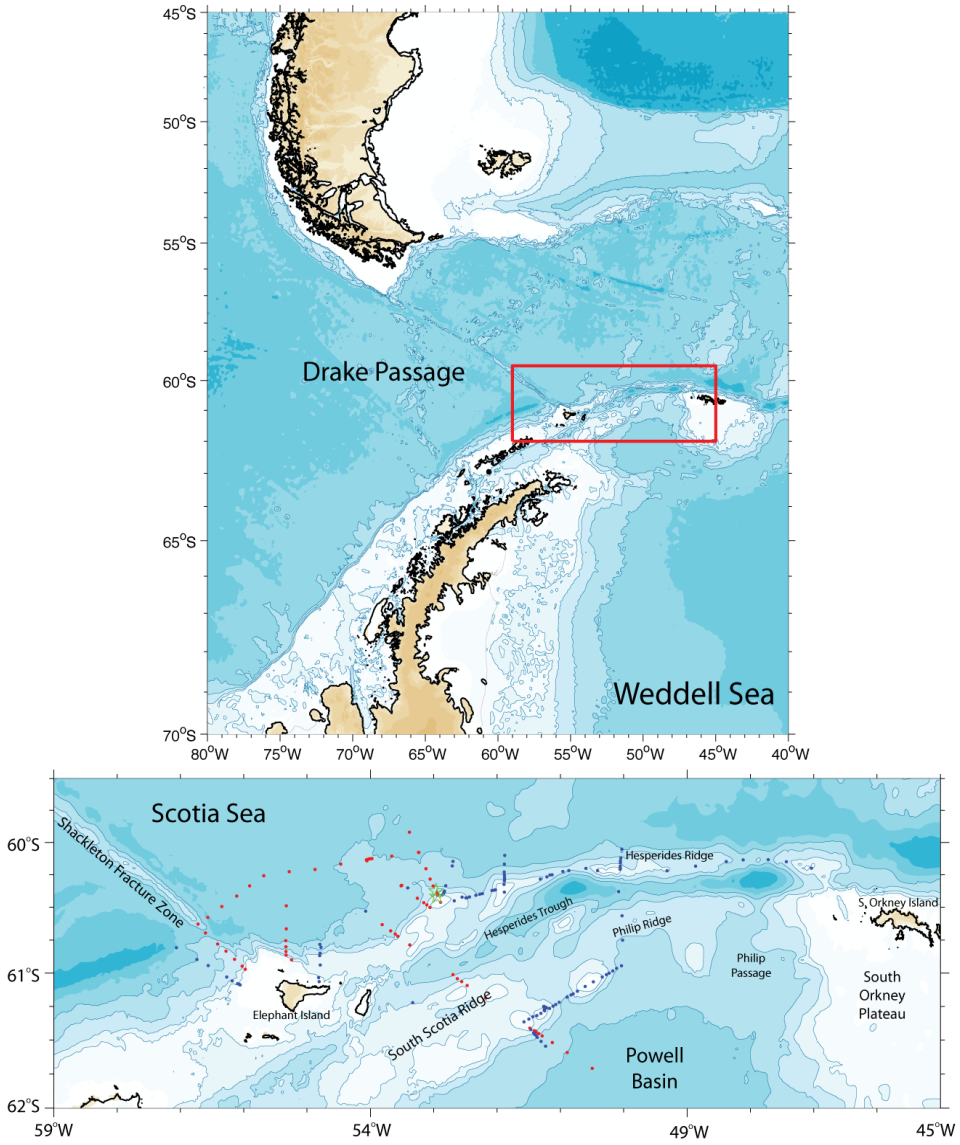


Figure 1. (top) Map of Study Area. Map of South Atlantic /Antarctic Peninsula region with the study area highlighted (red box). (bottom) Map of the study area with the locations of the moorings (green star), ACROSS CTD stations (red), and ESASSI CTD stations (blue) shown. Identifying bathymetric features and land masses are labeled. Isobaths are contoured every 500 m with shallower (deeper) regions in light (dark) blue.

**An overview of the Southern Ocean**

The global exchange of a wide-array of water masses in the Southern Ocean has a significant influence on large-scale oceanographic and climatological studies. In particular, new deep and bottom waters formed along the Antarctic continental slope margins extend far to the north contributing to global climate [*Whitworth et al.,* 1998]. Although restricted to the south by the Antarctic continent, the Southern Ocean's northern boundary is delineated by the uninterrupted eastward flow of the ACC.

*Antarctic Circumpolar Current*

The ACC is a strong and deep wind-driven current that surrounds Antarctica connecting all three major ocean basins [*Orsi et al.,* 1999]. Since the ACC is essentially a zonal current, isopleths on maps of water mass properties are also nearly zonal within the ACC, even at great depths, although continental features and the complex bathymetry of the Southern Ocean significantly steer its flow path [*Talley et. al.,* 2010]. The ACC enters the southwest Atlantic from the southeast Pacific through Drake Passage, and it dramatically turns northward deflected by the South Scotia Arc. The northern branch against the South American continental slope forms a tight cyclonic loop called the Malvinas Current [*Orsi et. al.,* 1995], before the ACC continues to flow uninterrupted around the globe exchanging waters with the rest of the world ocean.

*ACC fronts*

The Southern Ocean is characterized by a series of dynamical fronts that separate oceanic zones of distinct water mass stratification. The frontal paths are strongly controlled by the bottom topography. There are three prominent ACC fronts that can be identified as bands with large meridional gradients on vertical property distributions creating sharp transitions separating distinctive water properties in the upper layer. The Subantarctic Front (SAF) is situated near the northern edge of the ACC, the Polar Front (PF) lies within its center, and the southern ACC front (sACCf) near the southern periphery [*Orsi et. al.,* 1995].

*Antarctic Slope Current*

The ASC is located south of the ACC and flows in the opposite direction, i.e. mostly toward the west. In the Atlantic sector of the Southern Ocean the ASC transports approximately 50% of the waters that circulate within the subpolar Weddell Gyre [*Heywood et al.,* 2004]. In the western Weddell Sea the ASC flows northward following the upper portion of the continental slope, until it reaches the South Scotia Ridge (SSR) [*Heywood et al*., 2004]. After seeping through the SSR the ASC turns west toward the Drake Passage as it encounters the ACC to the north in the southwestern Scotia Sea. It is at this cross-road that the injection of Weddell Sea slope waters can effectively ventilate the intermediate and deep waters of the ACC. Understanding the extent of the local current interactions and offshore export of ventilated upper waters are the core of this study.

The Antarctic Slope Front (ASF) is associated with this current, which is crucial to understand for the scope of this study. The ASF is generally found near the shelf break. It separates the cold Shelf Water (SW) and Antarctic Surface Water (AASW) from warmer and saltier Lower Circumpolar Deep Water (LCDW) found offshore, creating a characteristic V-shape vertical density structure [*Whitworth et al.,* 1998].

*Circumpolar Deep Water*

Circumpolar Deep Water is the fundamental source water mass of the Southern Ocean [*Whitworth et al.,* 1998]. It lies vertically between the AASW and the Antarctic Bottom Water (AABW), and it is paramount for the mixing that occurs at the continental margins. It results from the mixing of deep waters incorporated into the bulk of Antarctic Circumpolar Current from all ocean basins. The Upper portion of CDW (UCDW) has an oxygen minimum core with source regions in the northern Pacific and Indian oceans, whereas Lower CDW (LCDW) is characterized by a salinity maximum derived from the northern North Atlantic [*Orsi et. al,* 1995].

*Antarctic Bottom Water*

Dense AABW is produced by convection at certain locations around the Antarctic margins, but most notably in the Ross and Weddell Seas. This water mass flows northward to replenish the abyssal layer of the world ocean, thus contributing to the global MOC. The outflow of AABW is restricted by the bottom topography and the flow

of the ACC [*Orsi*, 2010]. AABW formed at the continental margins of the Weddell Sea flows into the Scotia Sea through a deep narrow gap in the SSR called the South Orkney Gap [*Talley et. al.,* 2010].

*The Scotia Sea*

The Scotia Sea is the basin located east of the SSR and west of the Shackleton Fracture Zone (SFZ). Compared to the adjacent basins, the Scotia Sea is relatively shallow and its abyssal layer is filled with bottom water transported from the Weddell Sea. It is notorious for overall rough bottom topography and prominent ridge structures [*Locarnini et al.,* 1993]. Recently ventilated, cold upper waters carried by the ASC are exported at the SSR region separating the Weddell and Scotia seas. *Nowlin and Zenk* [1988] identified Weddell slope water flowing toward Drake Passage along the northern flank of the SSR. Here they distinguished the ASF by the sharp property gradients found between the cold and fresh Antarctic Slope Water inshore and the warm and salty CDW offshore [*Locarnini et al.,* 1993]. Therefore the rapid ventilation of the ACC at its cross-road with the ASC at the western SSR provides a dynamic connection between the upper waters of the Weddell Sea and the abyssal layer of the world ocean.

**Previous and current research programs in the study area**

The Deep Ocean Ventilation Through Antarctic Intermediate Layers (DOVETAIL) experiment (1997 – 1998) was an international program that studied the path and transport of AABW from the Weddell Sea to the ACC [*Muench and Hellmer,* 2002].

After the UK ALBATROSS experiment (2000) the most commonly cited mechanism is the rapid upward diffusion of properties from the densest waters that flow out from the northern rim of the Weddell Gyre [*Naveira Garabato et. al.,* 2004]. These waters (orange paths in Figure 2) flow east along the southern flank of the SSR, around the South Orkney Plateau through deep troughs, then west along the northern flank of the SSR before spreading into the Scotia Sea.

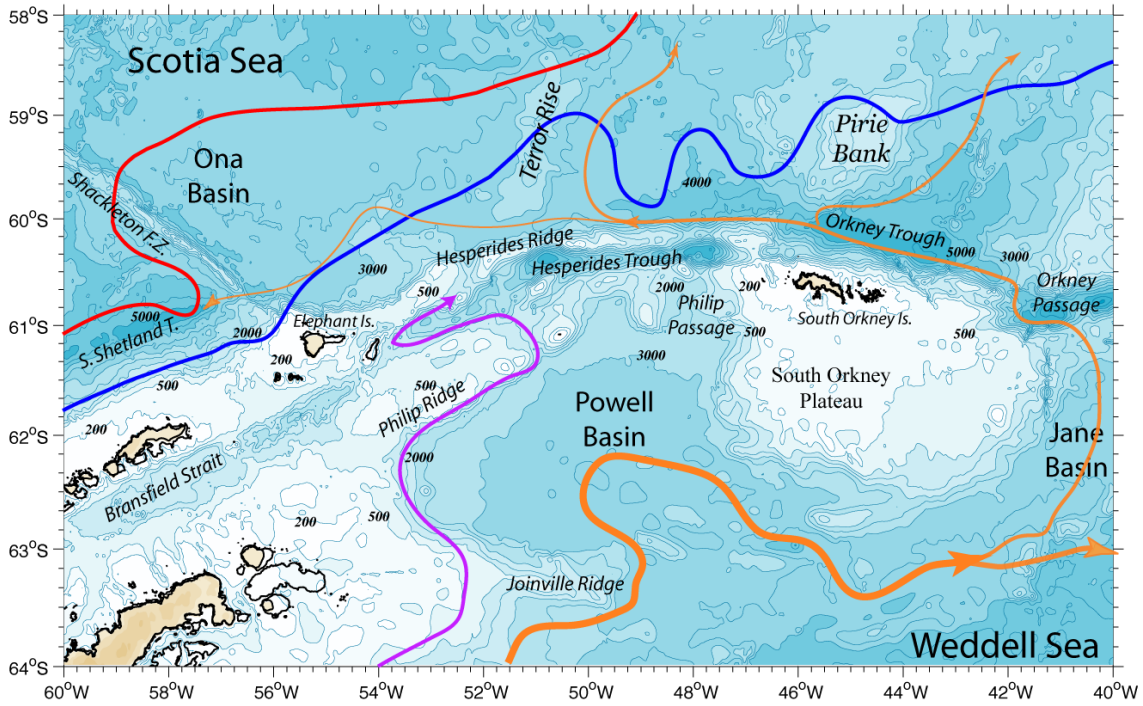


**Figure 2.** Study Area Location. Study area with color lines indicating the approximate paths of the southern front (red) and boundary (blue) of the ACC and the ASC (purple) and the outflow of the densest AABW (orange).

The Antarctic CRossroad Of Slope Streams (ACROSS) project was lead by Dr. Orsi with funds from the National Science Foundation (NSF) as a U.S. contribution to the Synoptic Antarctic Shelf-Slope Interactions (SASSI; http://sassi.tamu.edu) study of the

International Polar Year (IPY). Observational components consisted of a cruise onboard the Argentine *B.O. Puerto Deseado* (17 February – 12 March, 2009) and the deployment of two sub-surface moorings at the northern flank of the SSR between February 2009 and 2010 [*Orsi,* 2009]. The choice for the mooring array location near 53°W was based on the *RV Hesperides* 2008 cruise data, as best to sample the volume flux and properties of slope waters from the ASC that reaches the northern flank of the SSR.

The 2009 regional survey (Figure 3) occupied seven cross-slope transects with 57 closely-spaced hydrographic stations of full water column measurements of temperature, salinity, dissolved oxygen (CTD/DO) and lowered acoustic current profiling (LADCP); launched 60 Expendable Bathythermograph (XBT) probes; and deployed 20 satellite-tracked surface drifters. Cross-slope injection of ventilated upper waters to the deep ocean was successfully monitored during the full 1-year deployment (2009 – 2010) of two moorings, M1 at 600 m and M2 at 1800 m water depth, at the continental slope of the South Scotia Ridge. This array (Figure 4) included a total of 14 current meters, and 22 Temperature-Conductivity-Pressure (TCP) recorders provided high vertical resolution below 300 m [*Walpert and Orsi,* 2010].

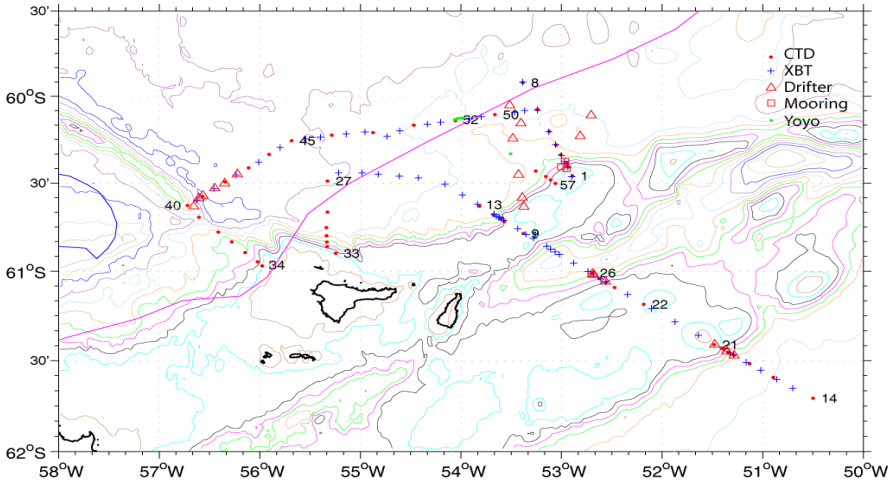


**Figure 3.** ACROSS Regional Survey. Location of all measurements taken during the ACROSS 2009 cruise. CTD casts (red) and yoyo CTD casts (green) are shown by dots. XBT probe launch locations are shown by the blue plusses. The deployment locations of the 3 moorings (red squares) and surface drifters (red triangles) are also shown.

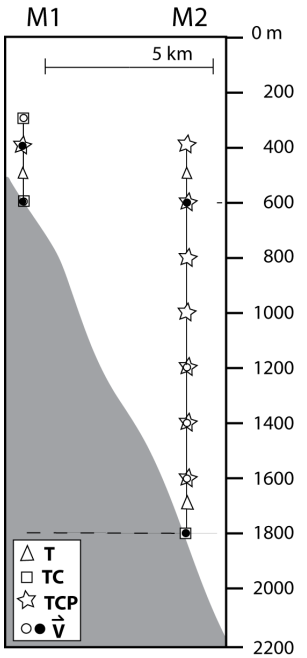


**Figure 4.** Moored Instrument Schematic. The vertical locations of CTP sensors (triangles/squares/stars) and Nortek (solid circles) and Aanderaa (open circles) current recorders are shown.

This study will analyze these newly collected hydrographic data and time series from moored instruments in the Weddell-Scotia region collected during the ACROSS field program [*Orsi,* 2009]. These two data sets are complementary. The cross-slope transects of closely spaced stations (~2 – 10 km) resolve the narrow Antarctic Slope Current, ASF, and the outflow of newly ventilated Weddell slope waters at the time of the cruise. Figure 5 shows the cross slope section near 53°W. Relatively steep sloping isopycnals found between stations 3 and 4 with a water depth around 600 m are indicative of the westward flowing ASC. The ASF characteristic separation of warm, salt waters from colder fresh water is also seen in this section between stations 5 and 6 where offshore waters saltier than 34.68 and warmer than 0.8°C are sharply separated by much colder ($\theta$ < 0.4°C) and fresher (S < 34.66) waters directly south. The time series from the ACROSS moorings are adequate to resolve the current's temporal variability over tidal to seasonal time scales.

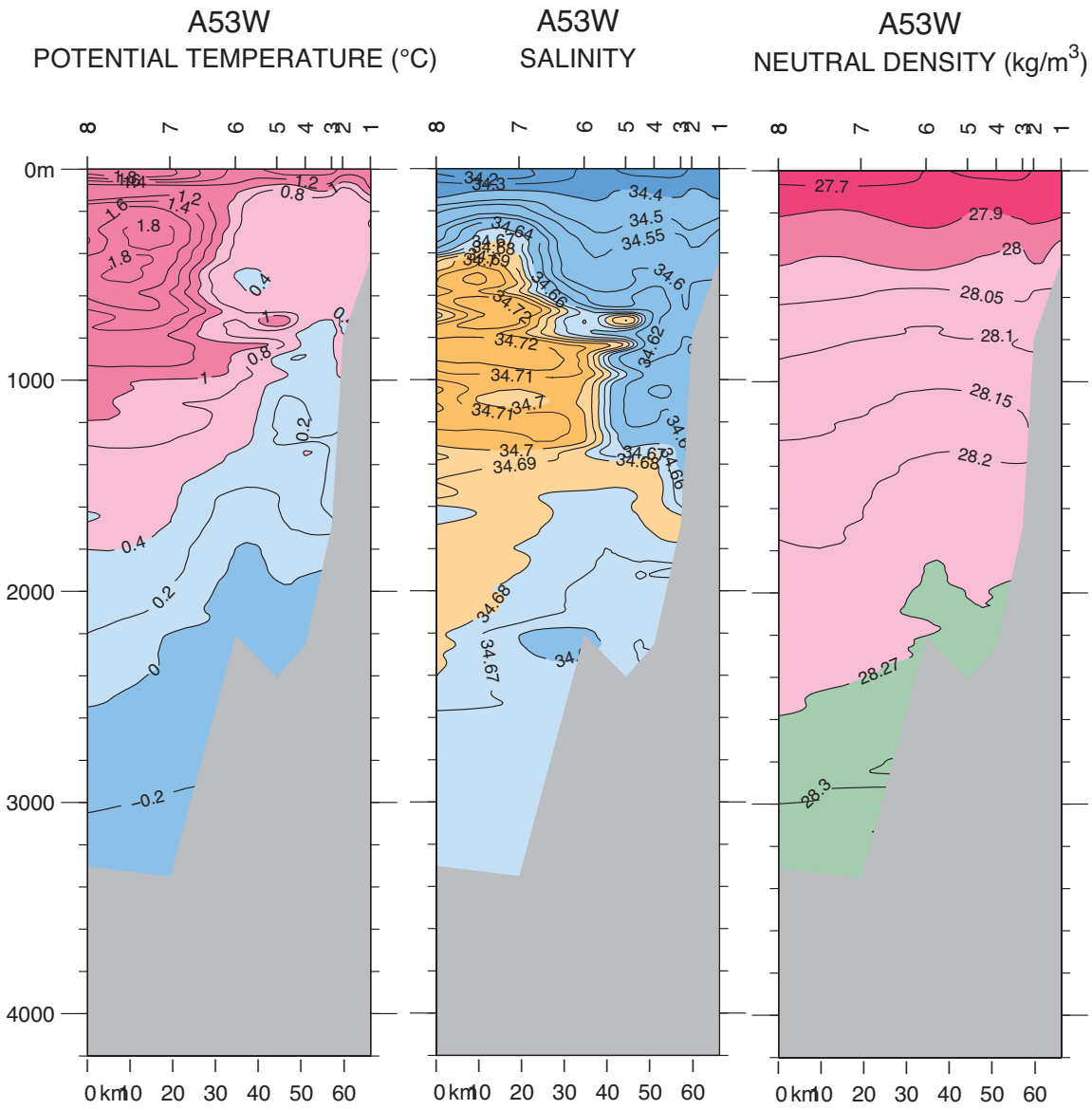


**Figure 5.** Vertical Sections for Hydrographic Stations near 53°W. Vertical sections of potential temperature (°C), salinity and neutral density (kg $m^{-3}$) for 2009 ACROSS hydrographic stations near 53°W along the northern flank of the SSR. The orientation of the sections is from north (station 8) to south (station1). The location of these stations can be seen in Figure 3.

The twofold objectives of this project are [A] to characterize the Antarctic Slope Current in the southwestern Scotia Sea as it interacts with the opposing Antarctic Circumpolar Current at the northern flank of the South Scotia Ridge; and [B] to determine the physical properties and volume transport of ventilated slope waters exported to the deep Scotia Sea. The governing hypothesis is that the localized rapid ventilation of the Antarctic Circumpolar Current is facilitated by mechanisms involving the slope frontal distribution and the associated intermediate-depth outflows of slope water. The alternative hypothesis is that significant intermediate-depth outflows of ventilated Weddell Gyre water from the Antarctic Slope Current are injected northward along isopycnal surfaces as a result of dynamic interactions between fronts and the complicated bottom topography [*Whitworth et. al.,* 1994]. Confirmation of this hypothesis would indicate that the ACC could respond more rapidly to seasonal-to-decadal variability in the Weddell Sea continental margins, where the dense water is produced, than if ventilation occurs solely through enhanced deep upward mixing offshore.

# CHAPTER II

# METHODOLOGY

## Mooring overview

Cross-slope injection of ventilated upper waters to the deep ocean was successfully monitored during the full 1-year deployment of two moorings, M1 at 600 m and M2 at 1800 m, with an array of direct current and temperature-conductivity-pressure (TCP) measurements. The ACROSS mooring array (Table 1) was deployed in February 2009, and two of them were recovered at the end of January 2010. Each mooring was deployed ~ 5 – 10 km apart at specific depths for the optimal characterization of the ASC and its interactions with the ACC. This moored array was instrumented with a total of 9 (5 additional were lost) current meters and 14 (8 more lost) TCP recorders placed ~ 100 – 200 m apart on the mooring line to ensure a high vertical resolution below 300 m. The vertical distribution of instruments in the two moorings adequately resolved the characteristic subsurface property gradients of the ASF.

## Time series

The primary data used in this study are moored time series measurements of temperature, conductivity, pressure and currents. Instruments measured slope waters at the expected depths on their way to Drake Passage farther to the west, or exported northward during frontal fluctuations interacting with the local topography of the slope.

M1 was outfitted with three Sea-Bird Electronics (SBE) MicroCAT 37 sensors nominally at 300 m, 400 m, and 600 m to measure temperature, conductivity and pressure (TCP) or just TC, one SBE MicroCAT 39 sensor at about 500 m to measure temperature, and three current meters. M1 had two different current meter instruments: one Aanderaa RCM7 mechanical current meter at 300 m and two Aquadopp-2000 acoustic current meters at 400 m and 600 m to measure velocity data. M2 was equipped with eight SBE MicroCAT 37 sensors and two Sea-Bird MicroCAT 39 sensors, as well as two Aanderaa RCM7s, two Aanderaa RCM8s, and two Aquadopp-2000 current meters (Table 1). These instruments collected data every 30 minutes.

SBE MicroCAT instruments collect the most accurate TCP readings, but not all the recorders were equipped with all of these sensors. The SBE39 is only a temperature recorder, while the SBE37 collects T, C and P or just T and C if close to the ocean floor. Current meters, either the mechanical Aanderaa (aa) or the acoustic Nortek instruments (no), record current speed and direction, and some also T, C and P. The precision of the TCP sensors on the mechanical current meters (RCM-7 or RCM-8) is not as accurate as that in the MicroCATs, and therefore will not be used in this analysis. The accuracy of the TP sensors on the acoustic current meters (Aquadopp-2000) is comparable to the MicroCATs, as it will be shown here (Figure 6) and is utilized when lacking T and/or P measurements at that respective depth.

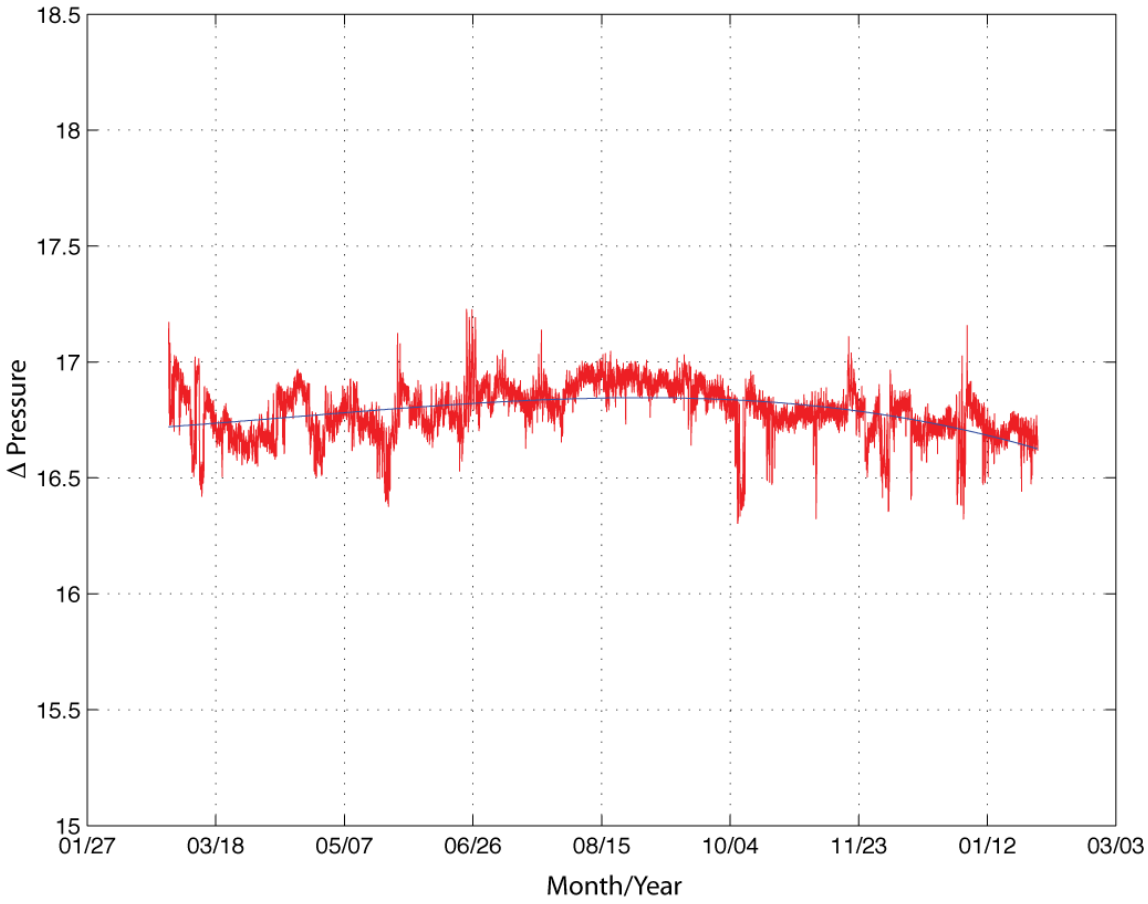


**Figure 6**. Pressure Offset between Paired Nortek Current Meter and MicroCAT. Pressure difference versus time between a paired Aquadopp-2000 (m2@600no) and SBE 37 (m2@600mc). The mean difference in pressure between the two instruments is 16.79 db. A third order polynomial fitting is shown by the blue line.

**Table 1.** ACROSS Moored Array[a]

| | | |
|---|---|---|
| M1 | | |
| 60°25.089'S | 52°57.025'W | 600 m |
| MCat (SBE37) | 272 m | CT* |
| CM (RCM-7) | 273 m | UVTCP |
| CM (AQD-2000) | 372 m | UVP |
| MCat (SBE37) | 372 m | TCP |
| MCat (SBE39) | 472 m | T* |
| CM (AQD-2000) | 572 m | UVP |
| MCat (SBE 37) | 573 m | CT* |
| M- | | |
| Not recovered | | |
| 60°24.338'S | 53°0.287'W | 1200 m |
| MCat (SBE37) | 300 m | TCP |
| MCat (SBE37) | 400 m | TCP |
| CM (AQD-2000) | 400 m | UVP |
| MCat (SBE39) | 500 m | T |
| MCat (SBE37) | 600 m | TCP |
| CM (AQD-2000) | 600 m | UVP |
| MCat (SBE37) | 800 m | TCP |
| CM (RCM-7) | 800 m | UVTCP |
| MCat (SBE37) | 1000 m | TCP |
| CM (RCM-7) | 1000 m | UVTCP |
| MCat (SBE39) | 1100 m | T |
| MCat (SBE37) | 1200 m | TCP |
| CM (RCM-9) | 1200 m | UVTCP |
| M2 | | |
| 60°22.530'S | 52°57.774'W | 1800 m |
| MCat (SBE37) | 428 m | TCP |
| MCat (SBE39) | 533 m | T* |
| MCat (SBE37) | 639 m | TCP |
| CM (AQD-2000) | 640 m | UVP |
| MCat (SBE37) | 845 m | TCP |
| MCat (SBE 37) | 1065 m | TCP |
| CM (RCM-8) | 1066 m | UVTCP |
| MCat (SBE37) | 1280 m | TCP |
| CM (RCM-7) | 1281 m | UVTCP |
| MCat (SBE37) | 1493 m | TCP |
| CM (RCM-8) | 1494 m | UVTCP |
| MCat (SBE37) | 1707 m | TCP |
| CM (RCM-7) | 1708 m | UVTCP |
| MCat (SBE39) | 1791 m | T* |
| MCat (SBE37) | 1918 m | TC* |
| CM (AQD-2000) | 1919 m | UVP |

[a]Mooring; location, nominal bottom depth; instrument (type), nominal water depth, sensors. Measurements include east-west (U) and north-south (V) currents, temperature (T), conductivity (C), and pressure (P). All MicroCat (MCat) recorders had T sensors, whereas all Current Meters (CM) were equipped with U, V and P sensors. Instruments lacking a pressure sensor are denoted by the (*).

**Data reduction**

The time series data recovered from the mooring array were processed using MATLAB software version R2010b. The raw mooring data was first converted to the working MATLAB file format used by our buoy group. Using the post-calibration files received from Sea-Bird Electronics, the raw data were calibrated to improve data quality. Subsequent to calibration, the data corresponding to the deployment and recovery times were removed.

Next, all parameters in the time series were despiked. Error detection was determined by using a time-series presentation technique; it is the most appropriate way of looking at the data to determine spikes [*Emery and Thomson*, 1997]. The data was displayed using a running 4-day window with a third order polynomial curve fitting the data in the appropriate window. Any data values beyond 3σ (standard deviation) of the curve were displayed and flagged. By visual inspection, the flagged variable(s) were either discarded or kept. For each instrument, all parameters were examined simultaneously to ensure consistency, as it is important to know if spiked values in one parameter such as temperature, are correlated with the same feature in another parameter, such as conductivity. This procedure was used for velocity, pressure, conductivity and temperature.

Debris interference often causes fouling of instruments, and as a consequence there are gaps in the mooring dataset. Gaps shorter than six hours were filled by the linear

interpolation method. Whereas the gaps longer than six hours were replaced by single spectrum analysis, a technique that partitions the original time series as a function of frequency; it is a tool that utilizes the full time series to predict values in the gap. There were only two instruments that had gaps larger than 6 hours: one 32-hour gap in m2@1280mc, and 3 gaps in m2@1707mc of 20-hours, 23-hours and 90-hours respectively. Only one instrument failed to record for the entire record: m2@1708aa stopped recording at the end of September, eliminating the last four months of data. Instruments lacking key properties, such as pressure and conductivity, were assigned values by interpolation from properties above and below the instrument. Lastly water properties, like potential temperature ($\theta$), neutral density ($\gamma^n$) and salinity, were calculated based on the measured TCP. A 40-hour low pass filter and a 30-day filter were also applied to all of the ACROSS time series.

**Data products**

After quality control and data reduction, the fundamental time-series analysis will be conducted. This includes calculating record-length mean properties and currents and main statistics of the observed variability and the mean transports. Mesoscale variability in this region will be examined as well as the correlation between all instruments in the ACROSS array.

Long-term direct measurements from the ACROSS mooring array will characterize the mean and dominant scales of spatial and temporal variability associated with the ASC,

and they will also provide some time-domain context for interpreting the shipboard CTD/LADCP data from the 2009 *Puerto Deseado* hydrographic cruise. These data will provide new and unique information about the ASC to improve our knowledge of the circulation of cold and low salinity slope waters, also called Modified Circumpolar Deep Water (MCDW), that replenish the deep and bottom layers of the ACC – the main goal of this research project.

# CHAPTER III

# RESULTS

This section describes the physical properties and currents measured at the ACROSS mooring array through examination of a 1-year record of half-hourly sampled time-series. Long-term mean hydrographic conditions are investigated based on hand-contoured vertical sections of the water mass properties. The mean statistics and vertical distribution of currents are also presented, and examined in combination with the θ-S scatter from moored instruments and nearby CTD hydrographic stations from the ACROSS (2009) and ESASSI (2008) cruises.

Tidal components were removed from the half-hourly raw current data by applying a 40-hour low pass filter. Then inferences of the variable nature and coherence of the slope current are made from visual inspection of all the available moored time-series plotted together.

**Time series**

All records of potential temperature at moorings 1 and 2 are illustrated in Figure 7. At levels where only SBE 39 sensors were available, which did not measure conductivity (and thus salinity), potential temperature was calculated using an interpolated salinity fields from SBE 37 instruments immediately above and below. Salinity and neutral

density time-series data were calculated at levels with data from all the SBE 37 instruments. The salinity and neutral density time-series plots for M1 and M2 are shown in Figures 8-9. For clarity, offsets, denoted in the figure legends, were applied to all parameters except for neutral density to depict the entire water column at each mooring.

Current meter time-series for example the u (east/west) and v (north/south) velocity components are plotted for the entire record. Time-series velocity components u and v from Nortek and Aanderaa current meters are shown in Figure 10 for M1 and Figure 11 for M2.

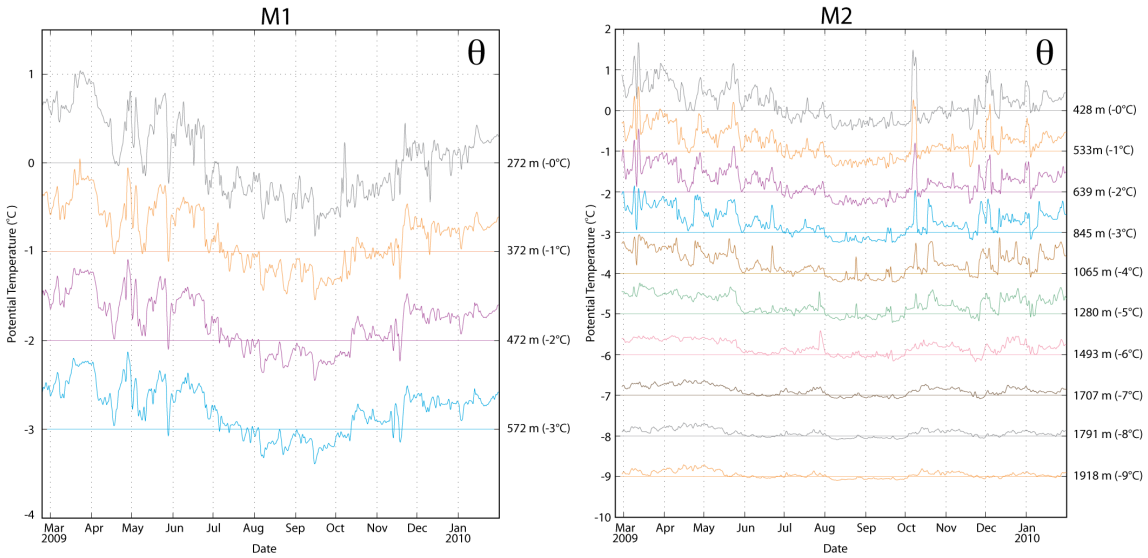


**Figure 7.** Potential Temperature Time-Series. Record length potential temperature versus time for M1 (left panel) and M2 (right panel) with a 40-h low pass filter applied to remove any tidal constituents. The mean depth of each instrument and temperature offset applied to the data are listed along the right-hand y-axis.

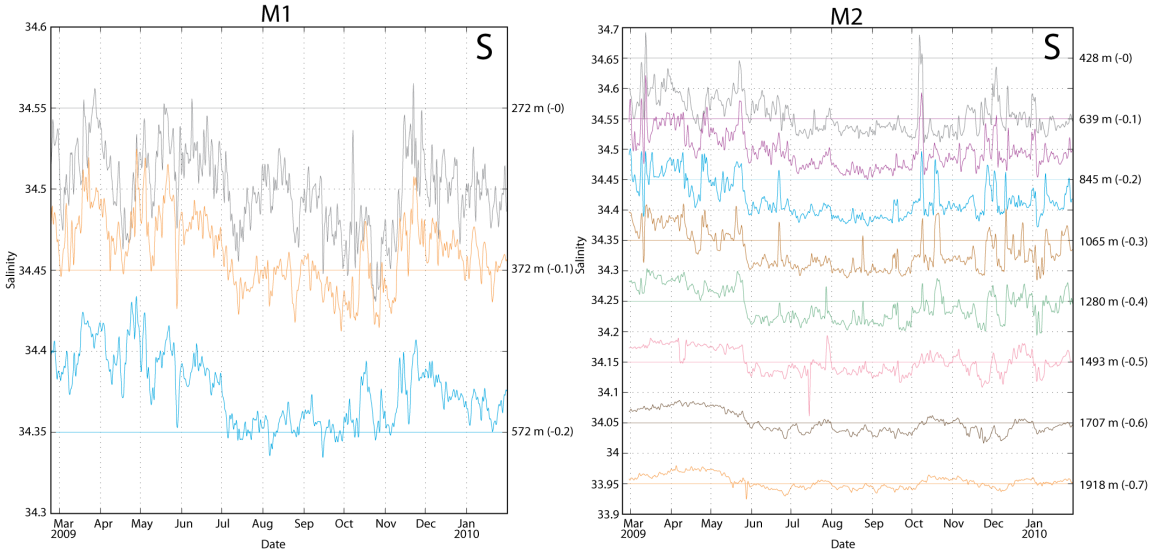


**Figure 8.** Salinity Time-Series. Record length salinity versus time for M1 (left panel) and M2 (right panel) with a 40-h low pass filter applied to remove any tidal constituents. The mean depth of each instrument and salinity offset applied to the data are listed along the right-hand y-axis.

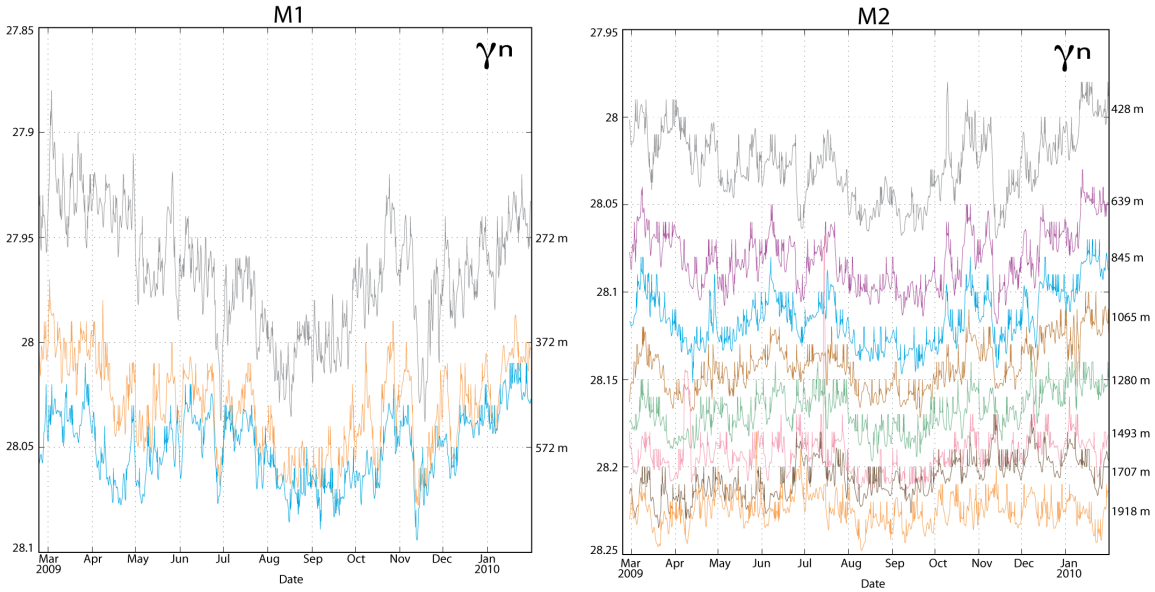


**Figure 9.** Neutral Density Time-Series. Record length neutral density versus time for M1 (left panel) and M2 (right panel) with a 40-h low pass filter applied to remove any tidal constituents. The mean depth of each instrument is listed along the right-hand y-axis. No offset was applied to these data.

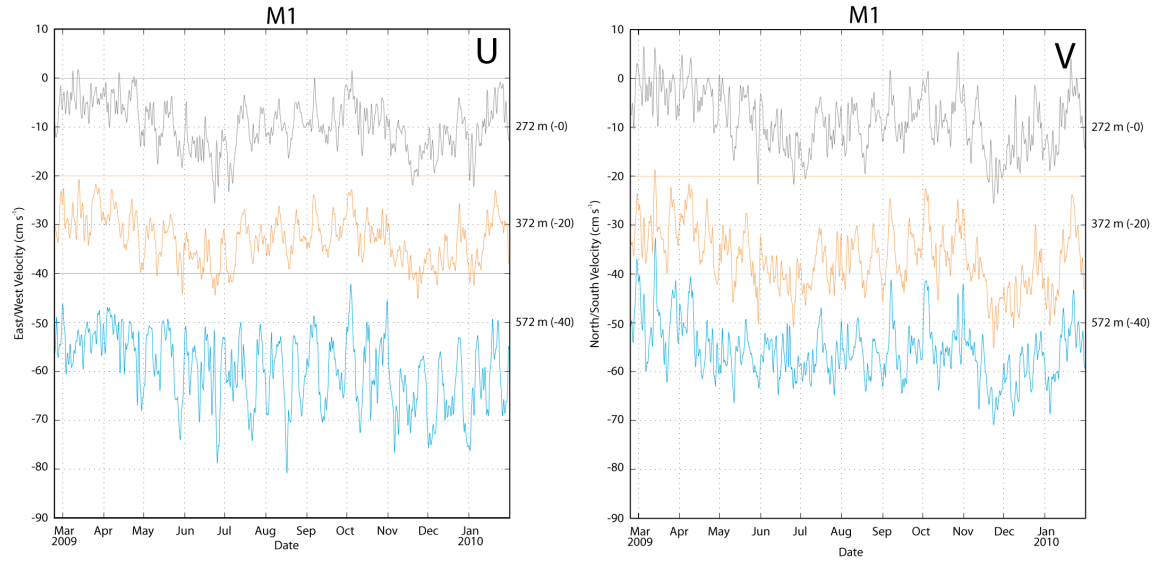


**Figure 10.** Mooring 1: Velocity Components U and V Time-Series. Record length velocity components u (left panel) and v (right panel) versus time for M1 with a 40-h low pass filter applied to remove any tidal constituents. The mean depth of each instrument and velocity offset in cm $s^{-1}$ applied to the data are listed along the right-hand y-axis.

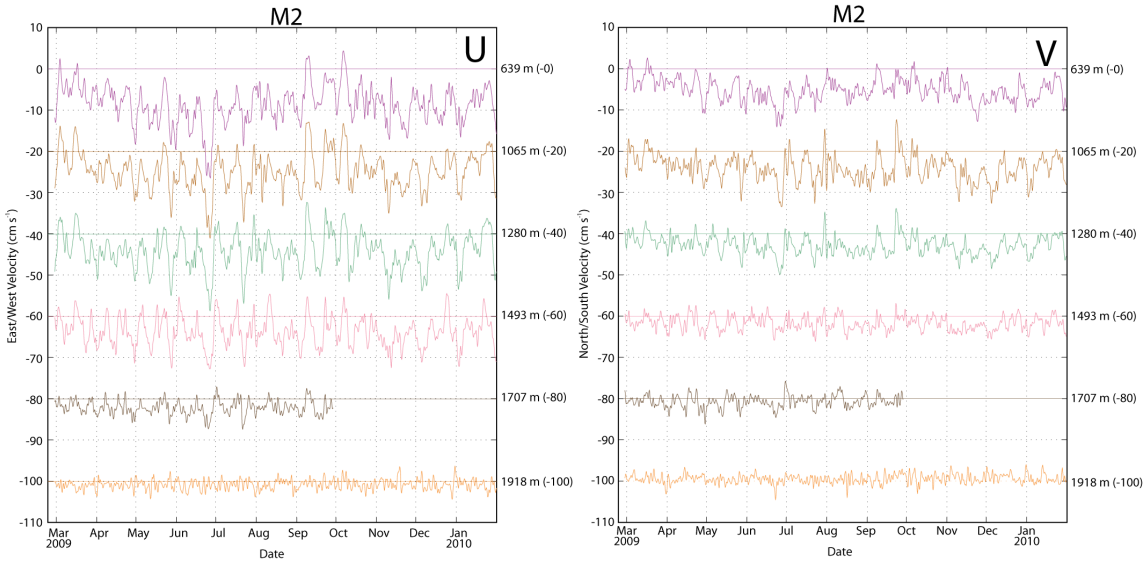


**Figure 11.** Mooring 2: Velocity Components U and V Time-Series. Record length velocity components u (left panel) and v (right panel) versus time for M2 with a 40-h low pass filter applied to remove any tidal constituents. The mean depth of each instrument and velocity offset in cm $s^{-1}$ applied to the data are listed along the right-hand y-axis.

**Power spectra analysis**

The conspicuous characteristic of the velocity components is the diurnal oscillation. The power spectra for the time series are shown in Figure 12. The spectra show energy frequencies in two small bands of diurnal and semidiurnal periods associated with the tides. The predominant tidal constituents are O1, K1 and M2. Diurnal components are O1 and K1 and semidiurnal component M2. There also appears to be two other tidal components, M3 cycling nearly three times a day, and the fortnightly MSF. The diurnal band exhibits the highest frequency.

**Long-term properties and currents**

Record-length mean water mass properties and velocity components for all instruments on M1 and M2 are presented in Table 2. A salinity field for instruments lacking conductivity sensors was derived from linear interpolation using instruments above and below. Mean salinity values for these instruments were not included in the table.

*Current properties*

The yearlong mean speeds for all current meters are presented in Table 3. Speed is computed by:

$$s = \sqrt{u^2 + v^2} \qquad (1)$$

The velocity at all moored current meters is predominantly southwestward, and due to the strong steering exerted by the local topography: the main orientation of the SSR is also northeast-southwest. On M1, the vertical structure of the mean flow shows that

bottom currents are on average not opposite to the surface currents, thus reflecting the barotropic nature of the Antarctic Slope Current. On M2 the strongest currents are found at sub-surface levels and diminish with depth. However at M1 inshore the opposite is true: the strongest currents are at the bottom (~ 600 m) where the mean zonal (meridional) velocity is about 20 cm $s^{-1}$ (16 cm $s^{-1}$) to the west (south). The mean bottom speeds (~ 1900 m) at M2 (6 cm $s^{-1}$) are five times slower than at M1 (30 cm $s^{-1}$).

The year-long mean velocity field is dominated by a strong (speeds > 20 cm $s^{-1}$) southwestward current at the upper slope parallel to the shelf break. This is the ASC carrying AASW mixtures from the Weddell Sea and Bransfield Straits toward Drake Passage.

*Physical properties*

General water mass properties over the continental slope are consistent with the characteristics of AASW and thermocline waters from the Bransfield Straits. The temperature minimum ($\theta < 0.1^{\circ}C$) at 300 m falls within AASW ($\gamma^n < 28$ kg $m^{-3}$). At mid-depths, the temperature maximum characterizes CDW at depths between 600 m and 1000 m with colder ventilated deep waters found below (~ 1900 m). The coldest measured waters are located near the sea surface, Antarctic Surface Water (AASW), and along the bottom of the slope, Weddell Sea Deep Water (WSDW).

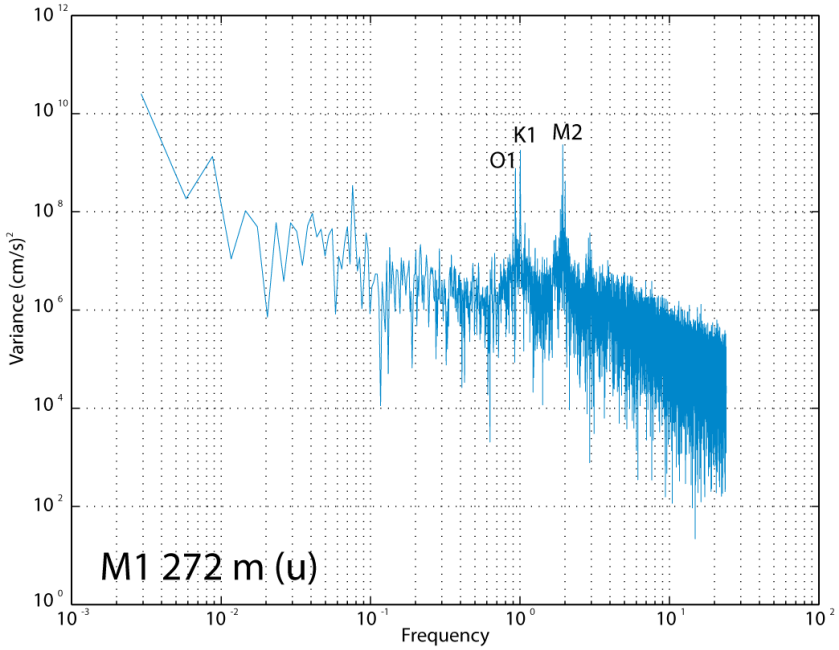


**Figure 12.** Power Spectra of M1 at 272 m. Power spectra of east/west (u) velocity component (frequency is cycles per day). Diurnal (O1 and K1) and semidiurnal (M2) tidal constituents are indicated.

**Table 2.** Record Length Mean Statistics[a]

| Mooring | Depth | Potential Temperature | | Salinity | | Neutral Density | | U | | V | |
|---|---|---|---|---|---|---|---|---|---|---|---|
| | | Mean | Std | Mean | Std | Mean | Std | Mean | Std | Mean | Std |
| **M1** | 272m | 0.062 | 0.42 | 34.501 | 0.02 | 27.968 | 0.02 | -9.645 | 4.92 | -8.558 | 5.85 |
| **M1** | 372m | 0.185 | 0.33 | 34.561 | 0.02 | 28.031 | 0.02 | -12.878 | 4.72 | -16.759 | 6.27 |
| **M1** | 472m | 0.213 | 0.29 | -- | -- | -- | -- | -- | -- | -- | -- |
| **M1** | 572m | 0.224 | 0.27 | 34.576 | 0.02 | 28.051 | 0.01 | -19.667 | 7.21 | -15.790 | 5.78 |
| **M2** | 428m | 0.174 | 0.40 | 34.557 | 0.03 | 28.028 | 0.02 | -- | -- | -- | -- |
| **M2** | 533m | 0.214 | 0.36 | -- | -- | -- | -- | -- | -- | -- | -- |
| **M2** | 639m | 0.241 | 0.34 | 34.598 | 0.03 | 28.081 | 0.01 | -8.513 | 4.56 | -5.156 | 2.77 |
| **M2** | 845m | 0.254 | 0.31 | 34.618 | 0.03 | 28.115 | 0.01 | -- | -- | -- | -- |
| **M2** | 1065m | 0.252 | 0.28 | 34.632 | 0.03 | 28.142 | 0.01 | -4.673 | 4.43 | -4.146 | 3.15 |
| **M2** | 1280m | 0.231 | 0.23 | 34.643 | 0.02 | 28.168 | 0.01 | -4.147 | 4.34 | -2.823 | 2.31 |
| **M2** | 1493m | 0.178 | 0.16 | 34.651 | 0.02 | 28.192 | 0.01 | -3.687 | 3.65 | -1.766 | 1.72 |
| **M2** | 1707m | 0.114 | 0.11 | 34.650 | 0.01 | 28.206 | 0.01 | -2.085 | 1.73 | -0.737 | 1.49 |
| **M2** | 1791m | 0.072 | 0.09 | -- | -- | -- | -- | -- | -- | -- | -- |
| **M2** | 1918m | 0.049 | 0.08 | 34.653 | 0.01 | 28.225 | 0.01 | -0.772 | 1.18 | 0.534 | 1.10 |

[a]Record-length mean statistics of 40-hour low pass filtered data. Values of potential temperature (˚C), salinity, and neutral density (kg $m^{-3}$) were determined from MicroCAT instruments. Values of velocities, u and v (cm $s^{-1}$) were determined using data from the current meter instruments (Nortek and Aanderaa).

**Table 3.** Record Length Mean Speeds[a]

| Mooring | Depth | Speed (cm $s^{-1}$) Mean | Std |
|---|---|---|---|
| **M1** | 272m | 20.2288 | 6.0976 |
| **M1** | 372m | 25.2177 | 7.0511 |
| **M1** | 572m | 29.8565 | 8.3340 |
| **M2** | 639m | 12.3202 | 4.0669 |
| **M2** | 1065m | 10.3147 | 3.4429 |
| **M2** | 1280m | 9.0205 | 3.0672 |
| **M2** | 1493m | 8.0763 | 2.6562 |
| **M2** | 1707m | 5.8791 | 1.9394 |
| **M2** | 1918m | 5.9817 | 1.9112 |

[a]Mean speed is calculated from the 40-hour low pass filtered zonal (u) and meridional (v) velocity components using Equation 1.

The record-length mean velocity, potential temperature (θ), salinity and neutral density ($\gamma^n$) fields are presented in vertical sections (Figures 13-16).

The record-length mean potential temperature, salinity, and neutral density ($\gamma^n$) fields are also shown in Table 2. The warmest average potential temperature on M2 occurs between 533 m and 1280 m indicating that these instruments are occupied by MCDW most of the time. The vertical section (Figure 14) shows a clear tongue of relatively warm water ($\theta > 0.25^{\circ}C$) with neutral densities between 28.05 and 28.15 kg $m^{-3}$. Mean bottom temperatures drop below 0.1 $^{\circ}C$ at M2 (~ 1900 m). Mean salinity values increase with increasing depth in the water column. Note that for the bottom two instruments on M2, there is a notable decrease in the mean potential temperature and an increase in salinity. The highest recorded salinity values at 1900 m are ~ 34.77, with the highest neutral density value of 28.27 kg $m^{-3}$.

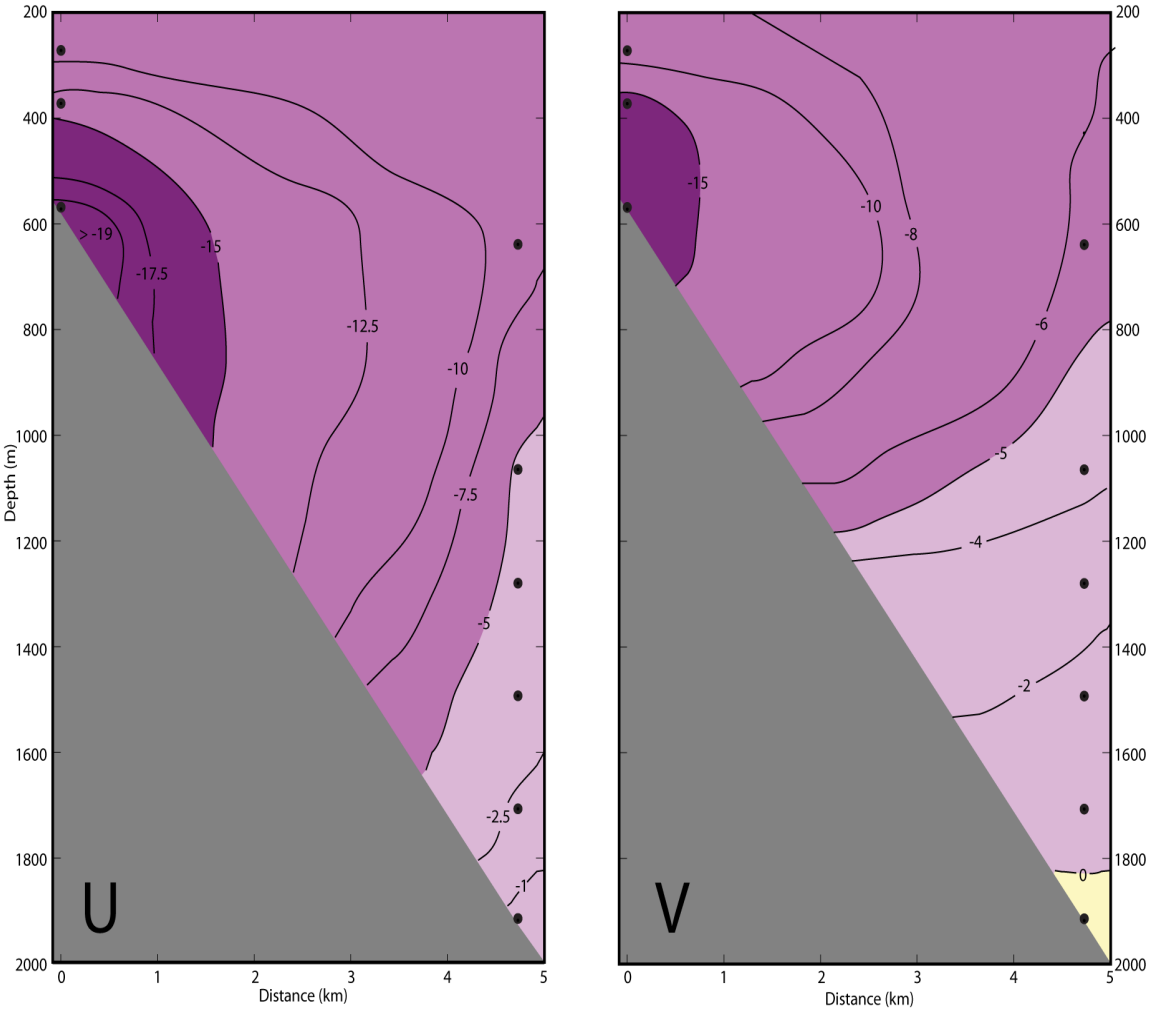


**Figure 13.** Velocity Components U and V Vertical Section. Vertical section of record-length mean velocity components (cm $s^{-1}$). (left) u-velocity component (east/west) and (right) v-velocity component (north/south). Negative velocities are shown in shades of purple while positive velocities are shades of yellow. The black circles show the mean depth of each current meter.

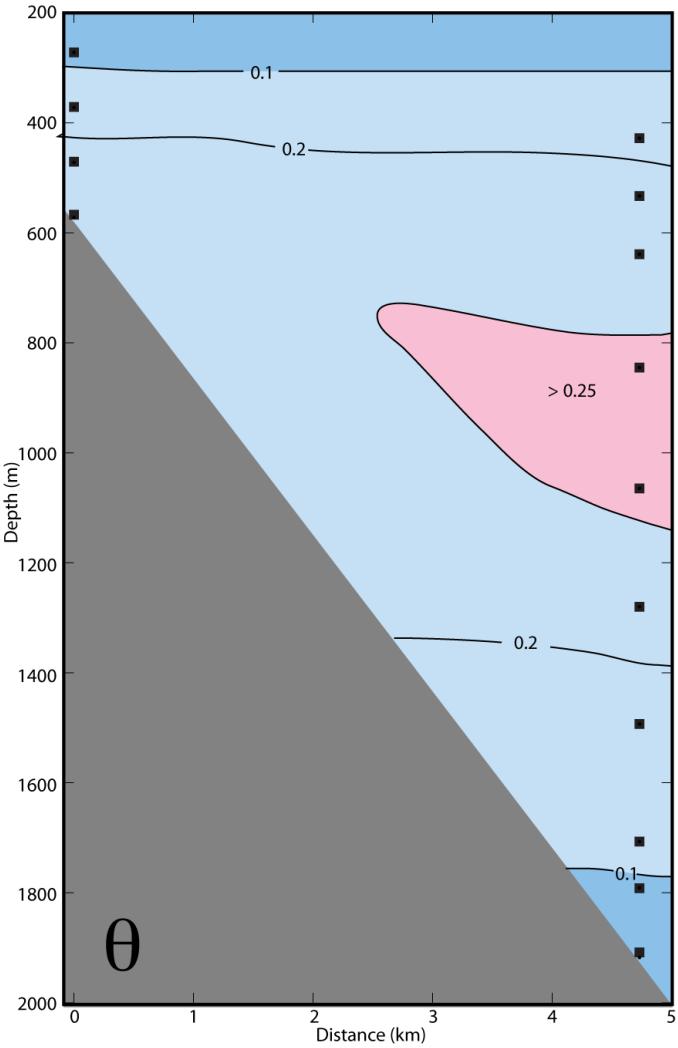


**Figure 14.** Potential Temperature Vertical Section. Vertical section of record-length mean potential temperature (˚C). The black squares show the mean depth of each MicroCAT.

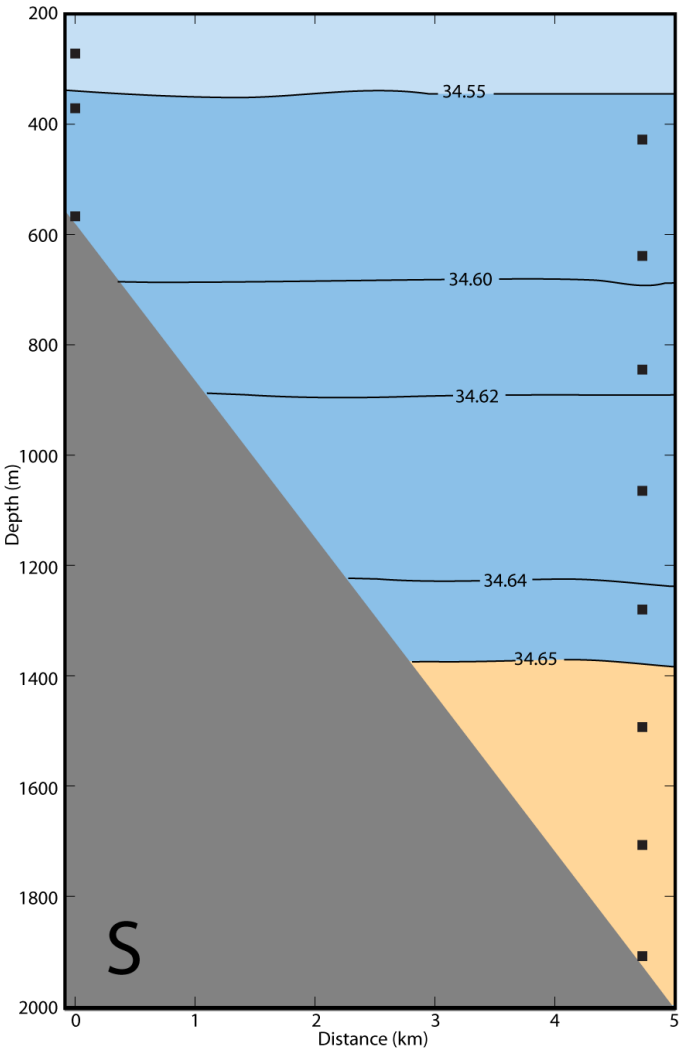


**Figure 15.** Salinity Vertical Section. Vertical section of record-length mean salinity. The black squares show the mean depth of each MicroCAT.

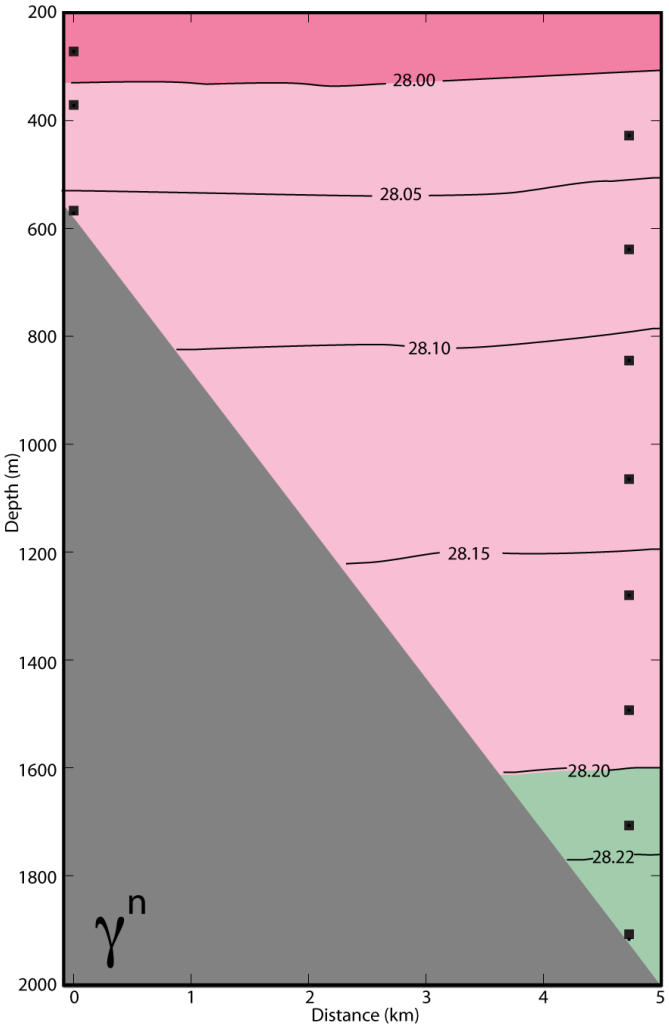


**Figure 16.** Neutral Density Vertical Section. Vertical section of record-length mean neutral density (kg $m^{-3}$) . The black squares show the mean depth of each MicroCAT.

# CHAPTER IV

# SUMMARY AND CONCLUSIONS

Physical properties and current measurements were used in this study of the Southern Ocean to improve our knowledge of the rapid ventilation of CDW in the ACC along the South Scotia Ridge. The eastward-flowing ACC interacts with the ASC that entered the Scotia Sea from the Weddell Sea across the western South Scotia Ridge [*Heywood et al.,* 2004]. The ASC is the dominant current at the moored array location as evident by the mainly southwestward flow found at both moorings. The most notable mixing that takes place in the Southern Ocean exists when the ACC encounters changes in the ocean floor topography [*Sloyan, B. M.,* 2005]. In the Scotia Sea, the mixing and modification of deep waters is contingent upon the complex bathymetry of the region [*Naveira Garabato et al.,* 2002]. For that reason, the spatial and vertical distribution of mixing near 53°W in the southern Scotia Sea is fundamental in understanding the processes involved in ventilating CDW and thus the abyssal global oceans. This rapid ventilation of the ACC in the Scotia Sea region is an important attribute of the MOC of the abyssal Southern Ocean.

## θ-S relationship

The high precision temperature and salinity data from the MircoCATs (SBE-37) are displayed as scatter plots of θ-S for filtered (Figure 17) and un-filtered (Figure 18) half-hourly data. Additionally, each θ-S plot has specific CTD stations from the ACROSS

(2009) and ESASSI (2008) cruises that were nearby the array location. The nearest stations to M1 are ACROSS station 2 (red line) and ESASSI stations 23 and 24 (blue lines); while the stations nearby M2 are ACROSS station 3 and ESASSI stations 21 and 22 (Figures 17 and 18). These figures reveal that the moorings captured considerably more variability in the area, versus a "snap-shot" in time from a CTD station.

The record-length means of potential temperature and salinity for each instrument are superimposed to the θ-S signature of selected ACROSS and ESASSI stations to show how the records spanned both regimes (Figure 19). Neutral density contours are displayed to distinguish and classify the various water masses, as indicated on the plots. The mean θ-S values from the array are warmer and saltier than stations 23 and 24 from the 2008 ESASSI cruise. The θ-S mean values are better reflected in the 2009 ACROSS CTD stations, although potential temperature in the upper water column is relatively lower in the moored array.

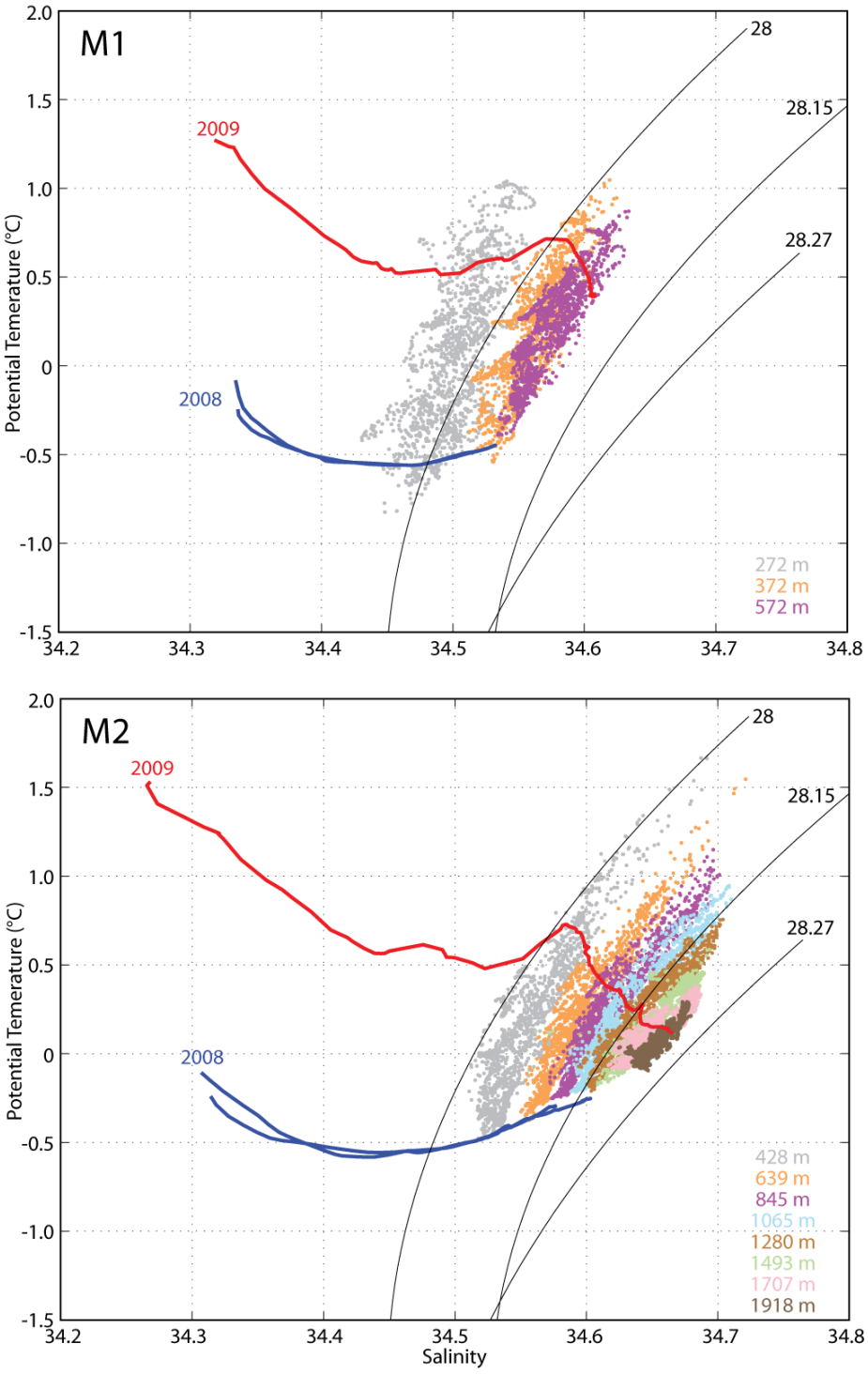


**Figure 17.** θ-S Relationship (Filtered) with CTD Stations from ACROSS and ESASSI. Record-length potential temperature and salinity relationship of 40-hour low pass filtered data for M1 (top) and M2 (bottom). CTD stations near the array deployment location collected during the ACROSS-2009 (red) and ESASSI-2008 (blue) cruises are shown by the thick lines. Selected neutral density isopycnals are shown by the black curved lines.

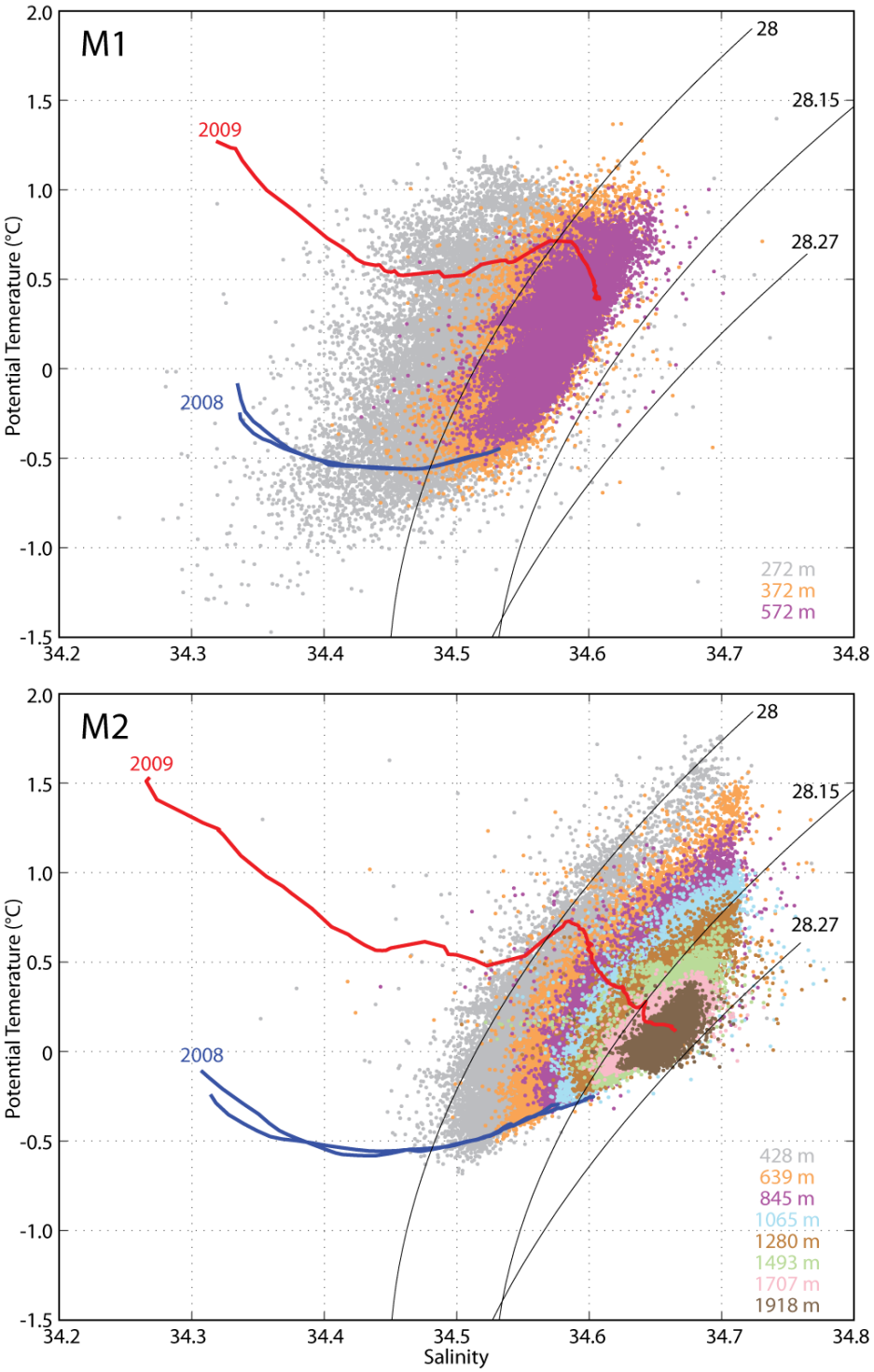


**Figure 18.** θ-S Relationship (Unfiltered) with CTD Stations from ACROSS and ESASSI Record-length potential temperature and salinity relationship of unfiltered data for M1 (top) and M2 (bottom). CTD stations near the array deployment location collected during the ACROSS-2009 (red) and ESASSI-2008 (blue) cruises are shown by the thick lines. Selected neutral density isopycnals are shown by the black curved lines.

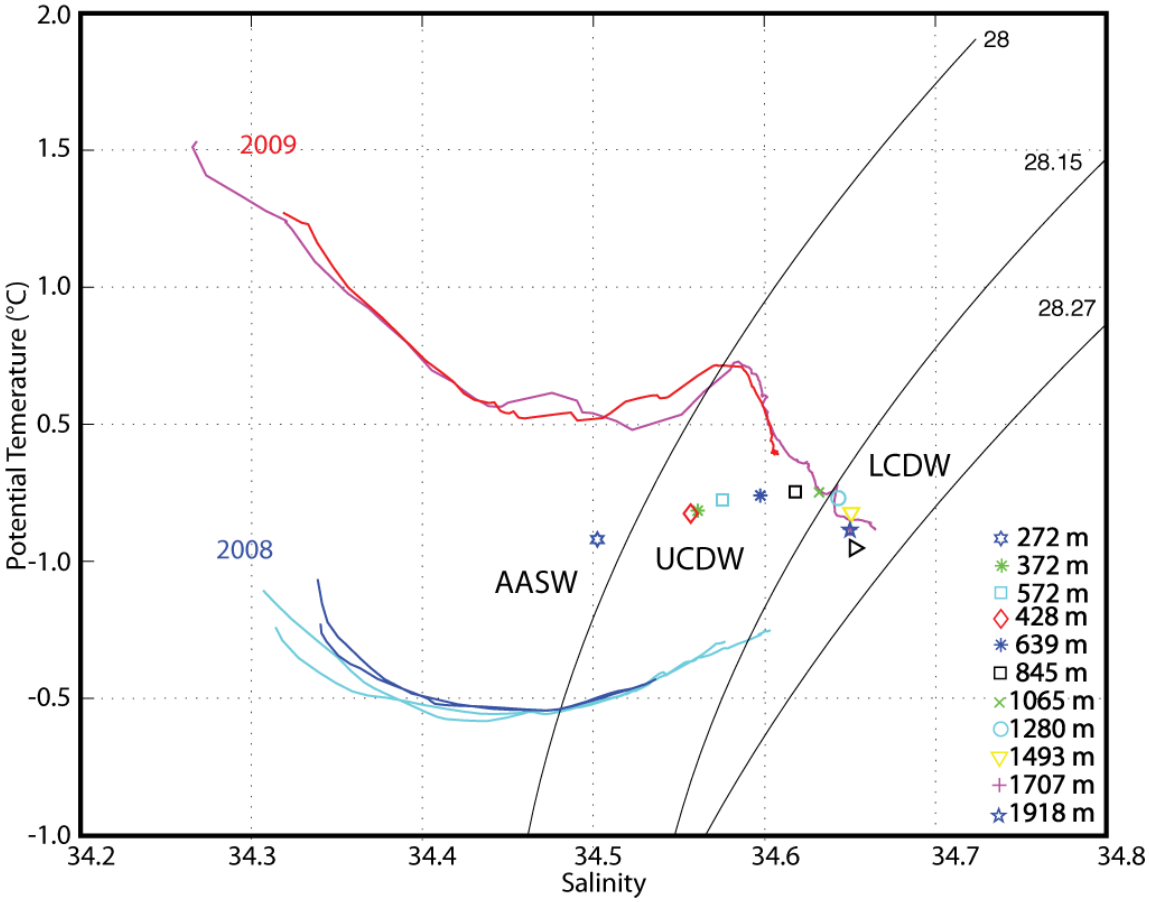


**Figure 19.** Record Length Mean θ-S Relationship. Potential temperature and salinity relationship (colored symbols) of 40-hour low pass filtered data for both moorings as listed in Table 2. CTD stations near the array deployment location collected during the ACROSS-2009 (red-M1, magenta-M2) and ESASSI-2008 (blue-M1, cyan-M2) cruises are shown by the thick lines. Selected neutral density isopycnals are shown by the black curved lines.

**Water mass properties**

The major water masses that flow within the study area are: Antarctic Surface Water (AASW), modified CDW (MCDW), and deep and bottom waters. Specific neutral density contours are used to define the water masses. AASW found above CDW and is marked by relatively cold temperatures ($\theta < 0.1^{\circ}C$) and low salinity ($S < 34.5$). Inflowing CDW mixes with this cold fresh water above and waters below resulting in MCDW. MCDW in this region is distinctive of a potential temperature maxima of $\theta > 0.2^{\circ}C$. Therefore, warm MCDW dominates the 500 – 1300 m layer along the SSR system. UCDW, identified by its temperature maximum and oxygen minimum core is classified with neutral densities between 28 and 28.15 kg $m^{-3}$; neutral densities between 28.15 and 28.27 kg $m^{-3}$ represent LCDW with a characteristic salinity maximum core. Deep and bottom waters (~ 1900 m) that occupy the location of the array include the mixing products of slope waters and remnants of CDW and are typically the coldest and densest waters found over the slope. The characteristics of this bottom layer ($\gamma^n > 28.15$ kg $m^{-3}$) are clearly indicative of MCDW being exported offshore along intermediate density layers. This water is lighter than AABW, it has Weddell Sea origin and it is transported to this location along the continental slope. Dense, bottom waters ($\gamma^n > 28.27$ kg $m^{-3}$) show sporadic westward export of Weddell Sea AABW.

A variety of water from the Weddell Sea is present over the slope region due to these waters circumnavigating the ridge system. Deep waters from the Weddell Sea seep through the SSR west of Orkney Passage occupying the southern portion of the Scotia

Sea [*Nowlin and Zenk,* 1988]. These waters that seep across the system through abyssal gaps in the bathymetry are cold, fresh and recently ventilated and move westward along the continental slope towards Drake Passage. However, previous studies indicate that most WSDW escapes the Scotia Sea and moves eastward [*Naveira Garabato et al.,* 2002]. These waters flow around the flank of the South Scotia Ridge and thus are distinguishable in both physical properties and current measurements recorded by the mooring array. Weddell Sea water that flows westward along the SSR system mixes with surrounding waters, further contributing to water masses variability in the region.

Frequency distributions of neutral density are important for determining the prevalence of AASW, UCDW, LCDW and bottom waters at certain locations in the water column (Table 4). AASW is found 84% of the time at 272 m. Over 90% of the record-length, UCDW is located at depths between 572 and 845 m and 85% of the time it is found at the 1065 m layer. LCDW is prominent at depths below 1493 m and is found 99.8% of the time at the 1919 m layer. Waters with densities greater than 28.27 kg $m^{-3}$ only occur 0.1-0.2% of the time, in the bottom layers nearest the continental slope (1065 – 1918 m).

**Table 4.** Frequency Distribution of Neutral Density Layers[a]

| Mooring | Depth | Neutral Density | | | |
|---|---|---|---|---|---|
| | | < 28.00 | 28.00-28.15 | 28.15-28.27 | > 28.27 |
| **M1** | 272m | 84 | 15.7 | 0.2 | 0.1 |
| **M1** | 372m | 22.6 | 77.4 | 0 | 0 |
| **M1** | 572m | 6.1 | 93.9 | 0 | 0 |
| **M2** | 428m | 24.1 | 75.8 | .1 | 0 |
| **M2** | 639m | 0.7 | 98.9 | 0.4 | 0 |
| **M2** | 845m | 0.2 | 98.5 | 1.3 | 0 |
| **M2** | 1065m | 0 | 84.9 | 15 | 0.1 |
| **M2** | 1280m | 0 | 29.6 | 70.3 | 0.1 |
| **M2** | 1493m | 0.1 | 2.6 | 97.2 | 0.1 |
| **M2** | 1707m | 0 | 0.2 | 99.7 | 0.1 |
| **M2** | 1918m | 0 | 0 | 99.8 | 0.2 |

[a]Neutral density (kg $m^{-3}$) values represent percentage of record-length time occupied by each water mass where $\gamma^n < 28.00$ is AASW, $28.00 < \gamma^n < 28.15$ is UCDW, $28.15 < \gamma^n < 28.27$ is LCDW, and $\gamma^n > 28.15$ is AABW. .

## Time series

Water mass variability can be depicted based on examination of physical properties and current changes. Record-length potential temperature and salinity time series from M1 and M2 show sufficient visual correspondence of variability (Figures 7 and 8).

The correlation between instruments on each individual mooring is clearly seen in the time series plots, as all moored instruments respond to similar signals throughout the water column (Figures 7-9). For instance, M2 potential temperature (Figure 7) has several large-amplitude peaks that are consistent with each subsequent deeper instrument, with amplitudes diminishing with depth. Additionally, the correlation between the two moorings, both M1 and M2, is evident by visual inspection.

These time-series show an apparent seasonal signal. Frequency distributions of potential temperature are important for further interpretation of water masses and mixing processes that occur near the slope. The bottom instruments on M2 (1493 – 1919 m) had the smallest temperature range distribution in comparison to shallower waters. Throughout the time-series, it is noted that large-amplitude oscillations are more prominent in March – May 2009, while oscillations with lower amplitudes occur during July – October 2009. The associated bottom water temperature is as cold as -0.095˚C in July, and then oscillates around 0.05˚C for the rest of the record length. In early October, the two shallow-most sensors of M1, 272 m and 372 m, show a peak in potential temperature, while the two deepest sensors, 472 m and 572 m, do not respond to such warming, suggesting a surface intensified event (Figure 7).

Intrusions of the ACC are depicted by large increases in potential temperature and salinity. There are four intrusions of CDW evident in the potential temperature and salinity time-series (Figures 7 and 8). The most prominent occurrence takes place in early October 2009 from 4 October until 15 October. During the time of this warm salty intrusion, current meters recorded northeastward flow, rather than the typical southwestward, further confirming ACC encroachment. The subsequent flow near the bottom is also northward, suggesting favorable conditions for export of bottom waters. During these events, CDW of the ACC impinges on bottom topography and MCDW results from enhanced mixing with surrounding waters. Consequently, as CDW exits the Scotia Sea it is notably cooler and fresher (MCDW) than prior entry to Drake Passage.

**Current velocity properties**

The current record shows a yearlong mean flow persistent in the southwestward direction. The semi-vertical banding demonstrated by the record-length mean velocity fields applies to velocity fluctuations over the slope (Figure 13). Current variability is attributed to the southwestward flowing ASC and the eastward flowing ACC. At mid-depths, current variability is the greatest. The bottom instrument at M2 (~ 1900 m) indicates semi-consistent flow; the mean east/west velocity component (-0.77 cm $s^{-1}$) and the mean north/south velocity component (0.53 cm $s^{-1}$) at 1918 m are significantly lower than at any other instrument. Throughout the record, the currents recorded in the bottom layer of M2 are visually not as dominant in direction as the upper part of the water column (Figure 20). This is validated by the smaller standard deviations (~ 1.5 cm $s^{-1}$) of the velocity components in the bottom two instruments (Table 2). At the bottom (572 m) of M1 the highest (-20 cm $s^{-1}$) mean east/west velocity is found for the entire array.

The potential temperature and salinity scatter plots recorded at M1 and M2 were also color-coded by velocity (Figure 21). These figures only include θ-S data that was paired with a current meter. At M1, AASW ($\gamma^n$ < 28 kg $m^{-3}$) flows predominantly southwestward, being carried by the ASC toward Drake Passage. The flow of UCDW ($\gamma^n$ = 28 – 28.15 kg $m^{-3}$) to a large extent is toward the southwest with sporadic events of north and west flows. LCDW ($\gamma^n$ = 28.15 – 28.27 kg $m^{-3}$) is dominated by northward and westward flow, intermixed with flow in the opposite direction. This is the attributed to CDW of the eastward moving ACC. When present, bottom waters ($\gamma^n$ > 28.27 kg $m^{-3}$)

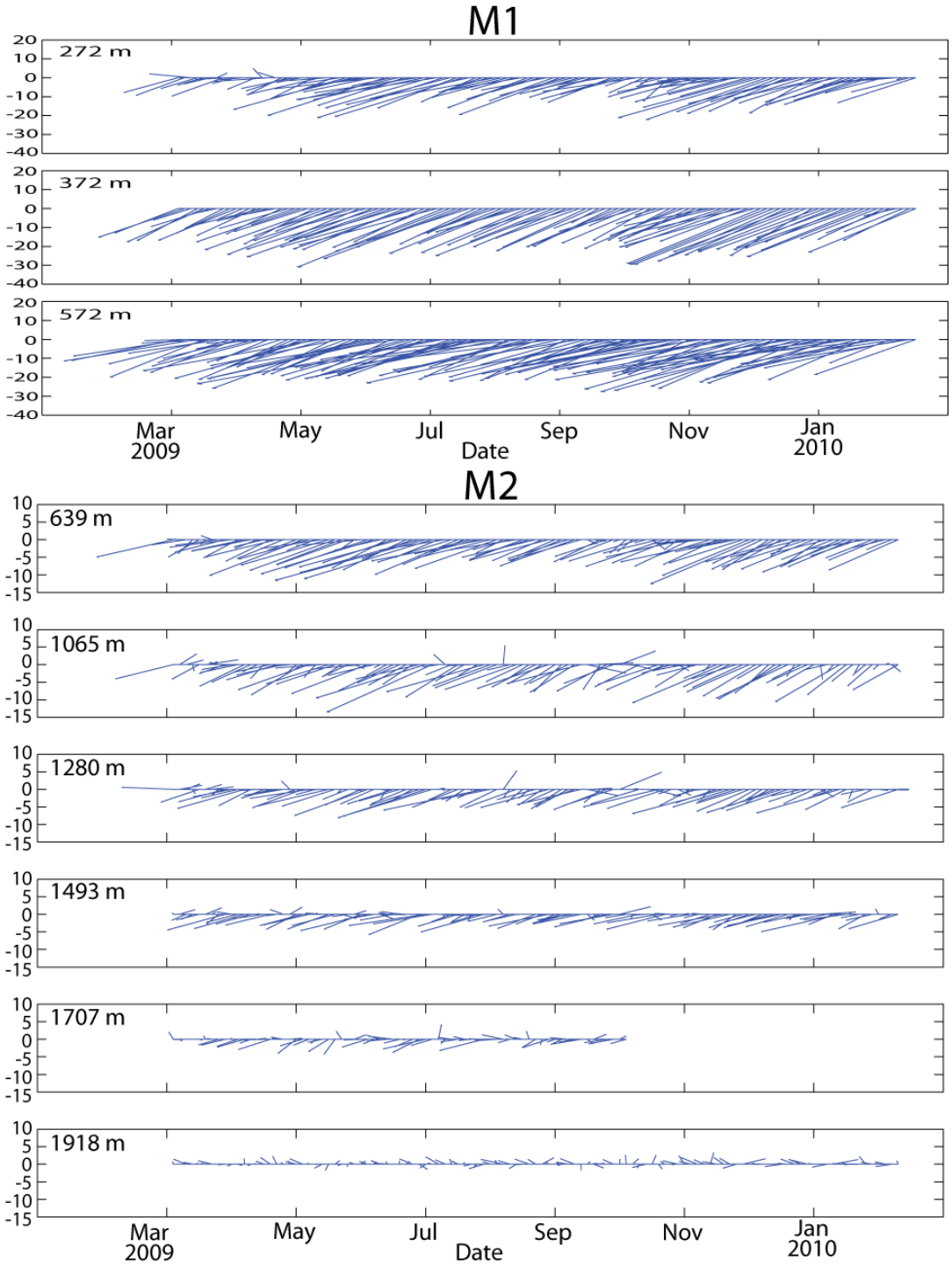


**Figure 20.** Current Vector Plot. Current vectors at 72-hour intervals for 40-hour low pass filtered data at M1 and M2.

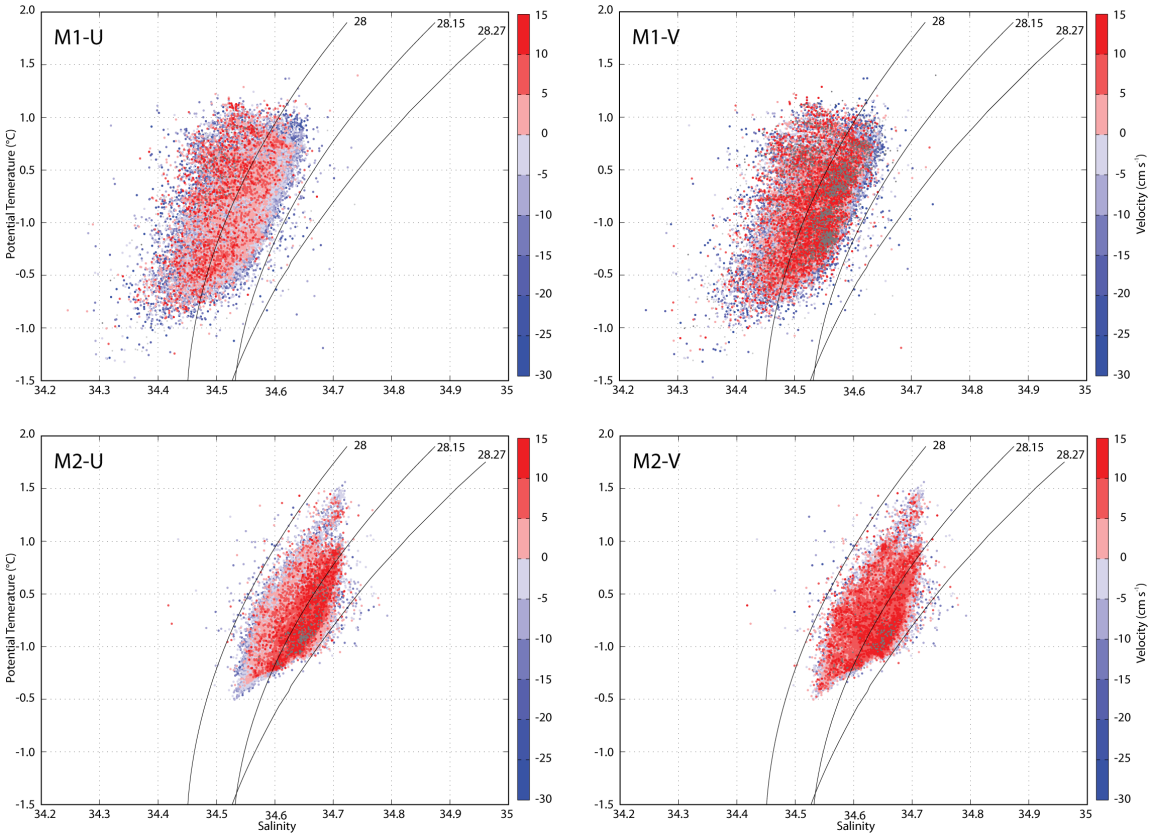


**Figure 21.** θ-S Relationship Color-Coded by Velocity. Potential temperature and salinity (θ-S) scatter plot color-coded by direction for the east/west (left panel) and north/south (right panel) velocity components recorded at M1 (top panels) and M2 (bottom panels). Positive velocities are shades of red while negative velocities are shades of blue. Selected neutral density isopycnals are shown by the black curved lines.

predominantly flow northeastward.

The overall direction of flow throughout the water column varies with depth, although southwestward flow along the SSR dominates the velocity field. The time-series depicts more variable zonal flow than meridional flow. At M1, the record length east/west velocity component records westward flow at depths between 300 – 600 m; while the flow of the north/south velocity component is predominantly southward, intermixed with a handful of northward pulses. At M2, the number of occurrences of eastward and northward flow, increase with depth in the water column. Throughout the record, the most episodes of eastward flow occur at bottom depths nearest the slope. Near the bottom of the continental slope at M2 (~ 1900 m), the number of northward events is more than double the southward flowing occurrences. At the array site, these events carry deep water originating from the Weddell Sea northward into the Scotia Sea

**Conclusions**

In conclusion, the identification of the mechanisms ventilating the ACC is important in improving our understanding on how the deep ocean is ventilated near the Antarctic coastal margins. The rapid cooling and freshening of the ACC is a pivotal process in the south Scotia Sea. ACC has the unique ability to export these recently ventilated waters throughout the global ocean and thus, the ACC has a significant role in the global MOC. The explanation of these mechanisms is expected to benefit future studies in determining climate-related changes observed in the colder coastal waters to the deep ocean.

# REFERENCES

Emery, W. K., and R. E. Thomson (1997). *Data Analysis Methods in Physical Oceanography.* Elsevier Science Inc., New York.

Heywood, K. J., A. C. Naveira Garabato, D. P. Stevens, and R. D. Muench (2004). On the fate of the Antarctic Slope Front and the origin of the Weddell Front. *Journal of Geophysical Research, 109*, C06021, doi:10.1029/2003JC002053.

Locarnini, R. A., Thomas Whitworth III, and W. D. Nowlin, Jr. (1993). The importance of the Scotia Sea on the outflow of Weddell Sea Deep Water. *Journal of Marine Research*, *51*, 135-153.

Muench, R. D., and H. H. Hellmer (2002). The international DOVETAIL program. *Deep-Sea Research II, 49*, 4711-4714, doi:10.1016/S0967-0645(02)00155-8.

Naveira Garabato, A. C., E. L. McDonagh, D. P. Stevens, K. J. Heywood, and R. J. Sanders (2002). On the export of Antarctic Bottom Water from the Weddell Sea. *Deep-Sea Research II*, *49*(21), 4715-4742, doi:10.1016/S0967-0645(02)00156-X.

Naveira Garabato, A. C., K. Polzin, B. A. King, K. J. Heywood, and M. Visbeck (2004). Widespread intense turbulent mixing in the Southern Ocean. *Science*, *303*(5655), 210-213, doi:10.1126/science.1090929.

Nowlin, W.D., and W. Zenk (1988). Westward bottom currents along the margin of the South Shetland Island Arc. *Deep-Sea Research*, *35*(2), 269-301, doi:10.1016/0198-0149(88)90040-4.

Orsi, A. H. (2009). Antarctic CRossroad Of Slope Streams expedition aboard B.O. Puerto Deseado in the southwest Atlantic Ocean February – March 2009, Technical Report 09-01-T, Texas A&M University, College Station, pp. 25.

Orsi, A. H. (2010). Recycling bottom waters, *Nature Geoscience, 3,* 307-309.

doi:10.1038/ngeo854.

Orsi, A. H., T. Whitworth III, and W. D. Nowlin, Jr. (1995). On the meridional extent and fronts of the Antarctic Circumpolar Current. *Deep-Sea Research I, 42*(5), 641-673, doi:10.1016/0967-0637(95)00021-W.

Orsi, A. H., G. C. Johnson, and J. L. Bullister (1999). Circulation, mixing, and production of Antarctic Bottom Water. *Progress in Oceanography*, *43*(1), 55-109, doi:10.1016/S0079-6611(99)00004-X.

Sloyan, B. M. (2005). Spatial variability of mixing in the Southern Ocean. *Geophysical Research Letters, 32*(L18603), 1-5. doi:10.1029/2005GL023568.

Talley, L. D., G. L. Pickard, W. J. Emery, and J. H. Swift (2010). *Descriptive Physical Oceanography: An Introduction (6th edition).* Elsevier Science Inc., Boston.

Walpert, J. N., and A. H. Orsi (2010). Antarctic crossroad of slope streams expedition aboard B. O. Hesperides in the southwest Atlantic Ocean January – February 2010, Technical Report 10-01-T, Texas A&M University, College Station, pp. 25.

Whitworth, T., W. D. Nowlin, A. H. Orsi, R. A Locarnini, and S. G. Smith (1994). Weddell sea shelf water in the Bransfield Strait and Weddell-Scotia confluence. *Deep-Sea Research I*, *41*(4), 629-641. doi:10.1016/0967-0637(94)90046-9.

Whitworth, T., III, A. H. Orsi, S.-J. Kim, W. D. Nowlin Jr., and R. A. Locarnini (1998), Water masses and mixing near the Antarctic Slope Front, in *Ocean, Ice, and Atmosphere: Interactions at the Antarctic Continental Margin*, *Antarctic Research Series,* vol. 75, edited by S. S. Jacobs and R. F. Weiss, pp. 1-28, American Geophysical Union, Washington, D.C.

# CONTACT INFORMATION


| | |
|---|---|
| Name: | Melanie R. Thornton |
| Professional Address: | c/o Dr. Alejandro R. Orsi<br>Department of Oceanography<br>3146 TAMU<br>Texas A&M University<br>College Station, TX 77843 |
| Email Address: | aorsi@tamu.edu |
| Education: | B.S., Environmental Geoscience, Texas A&M University, May 2011<br>Undergraduate Research Scholar |